

## Spectroscopic techniques: II Vibrational spectroscopy and electron and nuclear spin orientation in magnetic fields

### 13.1 INTRODUCTION

In Chapter 12 it was established that the electromagnetic spectrum was a continuum of frequencies from the high energy  $\gamma$ -rays of nuclear origin to the long wavelength region of the radiofrequencies. The energy associated with the spectrum decreases as it is traversed from the high to low frequency regions, according to the rules of quantum theory. There is therefore no obvious logical dividing point where this overall spectrum may be split. The split presented in this text is one of convenience. The justification is purely pragmatic and is based on 'common practice'. The biologist or biomedical scientist, having isolated a 'new' material (compound), is faced, initially, with the requirement to identify this isolate. Amongst the spectroscopic and spectrometric techniques available, assuming sufficient pure material has been obtained, the first analytical procedures to be used would, in practice, involve the methods described in this chapter. There are two important reasons for this approach: first, a considerable amount of information is obtained from a 'single' analysis and, secondly, the techniques are non-destructive. In view of the latter reason, replicate analyses may be performed in many cases, to improve signal-to-noise ratios, and precious samples can be recovered that may then be subjected to other analytical investigations.

In Chapter 9 the mass spectrometric techniques are encountered. These techniques give information different from and complementary to the spectroscopic ones. They have the distinct advantage of being considerably more sensitive and hence the investigator, often faced with having too small a sample to make use of the spectroscopic techniques, is forced to use mass spectrometry. However, it is essential to recognise that the spectroscopic techniques give information that is not available from mass spectrometry alone. Also, a disadvantage with mass spectrometry is that the technique is destructive and some of the sample is lost during the analytical procedure, although, with the most sensitive systems now available, the loss is probably insignificant. In many situations the amount of sample destroyed during analysis is less than losses arising from sample transfer!

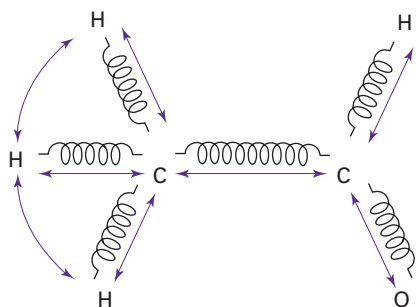


Fig. 13.1. Possible vibrations in acetaldehyde.

## 13.2 INFRARED AND RAMAN SPECTROSCOPY

### 13.2.1 Principles

With reference to the introductory statement of Section 13.1, the region of the electromagnetic spectrum, ranging from  $\gamma$ -rays to the near ultraviolet/visible (0.1–800 nm), contains frequencies that are sufficiently energetic to cause electron transitions, and the highest energy  $\gamma$ -rays are associated with nuclear transitions. From the near infrared region onwards there is insufficient energy to effect transitions of the kind alluded to above. Over the portion of the electromagnetic spectrum encompassing the range 0.8–25  $\mu\text{m}$  the phenomena involve ‘bond vibrations’. The term must be interpreted in a rather wider sense than just uniform oscillations and taken to include bending deformations as well.

#### Infrared and Raman

These two spectroscopic methods are complementary, giving similar information, but the criteria for the phenomena to occur are different for each type. It is also true that, for asymmetric molecules, absorptions will give rise to both types and virtually the same information could be gained from either. However, for symmetrical molecules having a centre of symmetry, the fundamental frequencies that appear in the Raman do not appear in the infrared and vice versa. The two methods are then truly complementary.

The reasons are the two different mechanisms on which the two types depend. Both are indicated in Fig. 13.1 for a simple molecule, acetaldehyde. For the purposes of this discussion the bonds between atoms can be considered as flexible springs so that the atoms are in constant **vibrational motion**, i.e. the molecule is not fixed and rigid.

Bonds can either **stretch or deform** (bend) and theory predicts that if a molecule contains  $n$  atoms there will be  $3n - 6$  fundamental vibrations in total. Of these,  $2n - 5$  cause bond deformations and  $n - 1$  cause bond stretching. In Table 13.1 are listed the most important fundamental frequencies observed in acetaldehyde molecules.

The region of the electromagnetic spectrum ranges from the red end of the visible to the microwave lengths. Energy is input by irradiating in the appropriate

**Table 13.1** Some fundamental frequencies associated with vibrations in acetaldehyde

Functional group	Vibration type	Frequency (cm <sup>-1</sup> )
- CH <sub>3</sub>	Bending	1460
		1365
- C - C -	Stretching	1165
- C = O	Stretching	1730
- C - H (in CH <sub>3</sub> )	Stretching	2960
		2870
- C - H (in CHO)	Stretching	2720

region with electromagnetic radiation. The criterion for an **infrared spectrum** is that there is a change in **dipole moment**, i.e. a change in charge displacement. Conversely, if there is a change in the **polarisability** of the molecule, a portion of the scattered radiation will have a frequency different from that of the incident radiation. These different frequencies constitute Raman spectra. It should be noted that more information can be gained about oscillations in molecules by proceeding even further into the microwave region and using **microwave spectroscopy**.

The fundamental frequencies observed are characteristic of the functional groups concerned and are absolutely specific. This gives rise to the term **finger-print** for the infrared pattern obtained. As the number of functional groups increases in more complex molecules, the absorption bands in the infrared patterns become more difficult to assign. However, **group frequencies** arise that help to simplify interpretation. These groups of certain bands regularly appear near the same wavelength and may be assigned to specific molecular groupings, just as particular chromophores absorb in the ultraviolet and visible regions. Such group frequencies are extremely valuable in structural diagnosis. It should be noted that, in infrared spectra, which are vibrational spectra, it is usual to work in frequency units, hertz (Hz), rather than wavelength.

The frequency associated with a particular group varies slightly, owing to the influence of the molecular environment. This is extremely useful in structural biochemistry studies as it is possible to distinguish between C - H vibrations in methylene (-CH<sub>2</sub>) and methyl groups (-CH<sub>3</sub>). Decrease in wavelength also occurs when double bonds are formed as the stretching frequency increases.

### 13.2.2 Instrumentation

The most common source is a Nichrome alloy coil heated to incandescence. This region of the electromagnetic spectrum contains the heat waves. Samples of solids are either prepared in mulls such as nujol and held as layers between salt planes such as NaCl or pressed into KBr discs. Non-covalent materials must be used for sample containment and also in the optics, as these materials are transparent to infrared.

Detectors are of the heat recognition type. The **Golay cell** contains gas or liquid whose expansion is registered when the energy is absorbed. Thermal detectors such as thermocouples can also be employed. Analysis using a Michelson interferometer allows **Fourier transform infrared spectroscopy** (FT-IR) to be performed. This instrument involves fixed and rotating mirrors that split the incident beam into two. The beams are recombined after passage through the sample but as the two pathlengths are different, interference patterns arise that may be analysed by Fourier transform methods (see Section 13.4.1 for consideration of FT methods). The Beer-Lambert law applies in all cases except complex mixtures, where more complicated mathematical procedures are required.

### 13.2.3 Applications

The use of infrared and **Raman spectroscopy** is mainly in biochemical research for intermediate-sized molecules such as drugs, metabolic intermediates and substrates. Examples are the identification of substances such as penicillin and its derivatives, small peptides and environmental pollutants. It is an ideal and rapid method for measuring certain contaminants in foodstuffs and can be coupled to a gas-liquid chromatograph (GC-IR) when it is also frequently used for the analysis of drug metabolites (Section 11.9.3). Fig. 13.2 shows the major bands of an FT-IR spectrum of the drug phenacetin. Gas analysis is rapid, particularly for measuring different concentrations of gases such as CO<sub>2</sub>, CO and CH≡CH (acetylene) in biological samples. Use in the study of photosynthesis and respiration in plants is valuable, particularly for CO<sub>2</sub> metabolism.

## 13.3 ELECTRON SPIN RESONANCE SPECTROSCOPY

### 13.3.1 Magnetic phenomena

Prior to any detailed discussion of **electron spin resonance** (ESR) and **nuclear magnetic resonance** (NMR) (Section 13.4) methods it is worth while considering the more general phenomena applicable to both.

An important consideration is magnetism and how it arises. All substances are magnetic, and magnetism arises from the motion of charged particles. This motion is controlled by internal forces in a system and, for the purposes of this discussion, the major contribution to magnetism in molecules is due to the **spin** of the charged particle.

Consider the situation in the chemical bonds of a molecule where electrons (negatively charged) have the property of spin controlled by strict quantum rules. The simplest view of the chemical bond is that of paired electrons with opposite spins. It is true that in many chemical systems the electrons may become delocalised, i.e. lose their association with a particular atom, but the essential argument still applies in that for pairs of electrons in molecular orbitals the spins must be opposite (no two electrons can have all the quantum numbers identical: the Pauli principle). Each of these spinning electronic charges generates a magnetic effect,

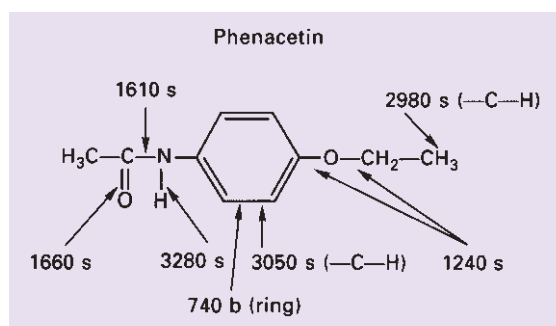
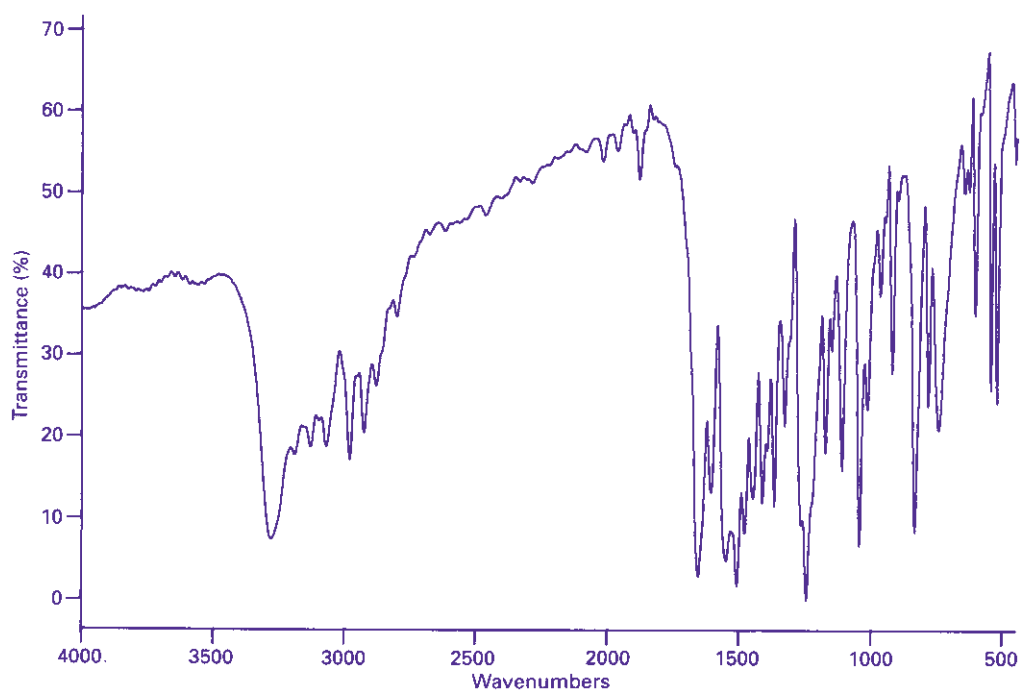


Fig. 13.2. FT-IR spectrum of phenacetin. Bands at the appropriate frequencies ( $\text{cm}^{-1}$ ) are shown, indicating the bonds with which they are associated and the type (s, stretching; b, bending or deformation).

but in electron pairs the effect is almost self-cancelling. The mathematical considerations do not in general apply exactly in molecules but in atoms a value for magnetic susceptibility may be calculated and is of the order of  $-10^{-6}\text{ g}^{-1}$ . This is **diamagnetism**, possessed by all substances because all substances contain the miniscule magnets, i.e. electrons. Diamagnetism is temperature independent.

If an electron is unpaired there is no counterbalancing opposing spin and the magnetic susceptibility is of the order of  $+10^{-3}$  to  $+10^{-4}\text{ g}^{-1}$ . In cases where this possibility arises, the underlying diamagnetism is so small by comparison that it

is irrelevant and the free electron case gives rise to **paramagnetism**. Free electrons can arise in a number of examples, the most notable of which is in the structure of certain metals such as iron, cobalt and nickel. These metals exhibit an extreme case of paramagnetism that is termed **ferromagnetism** and are the materials from which permanent magnets, with which everyone is familiar, can be made. Some crystal structures allow free electrons to exist but **free radicals** (free electron entities) are probably the most important systems in biological investigations.

The way in which a substance behaves in an externally applied magnetic field allows us to distinguish between diamagnetism and paramagnetism. A paramagnetic material is attracted by an external magnetic field and a diamagnetic substance is rejected. This principle is employed in the **GUOY balance**, which allows the quantification of the magnetic effects. A balance pan is suspended between the poles of a suitable electromagnet (to supply the external field). The substance under test is weighed in air with the current switched off. The same sample is then reweighed with the current on, the result being that a paramagnetic substance apparently weighs more and a diamagnetic substance apparently less.

Exactly similar arguments can be made regarding atomic nuclei. Of course, it is not now the extranuclear electrons but the subnuclear particles that are the spinning charged particles. Strictly speaking (because of interchangeability) it is the number of nucleons (protons plus neutrons) that determine whether a species will exhibit **nuclear paramagnetism**. It is beyond the scope of this discussion to explore why neutrons (which are neutral and uncharged; Section 14.1.1) are involved. It is sufficient to note that the hydrogen atoms in a molecule exhibit residual nuclear magnetism and, if some or all are replaced by deuterium, then there is no magnetism from the deuterium. Hydrogen contains a single proton, whereas deuterium contains one proton and one neutron (two nucleons, an even number). Carbon-12 ( $^{12}\text{C}$ ) contains six protons plus six neutrons – an even number, no residual magnetism.  $^{13}\text{C}$  contains six protons (because it is carbon) but seven neutrons, an odd number of nucleons; hence it exhibits residual nuclear magnetism.

### 13.3.2 The resonance condition

In both ESR and NMR techniques (Section 13.4) two possible energy states exist for either electronic or nuclear magnetism in the presence of an external magnetic field:

- *Low energy state  $E_1$* : The field generated by the spinning charged particle lies with, or is **parallel** to, the external field.
- *High energy state  $E_2$* : The field generated by the spinning charged particle lies against, or is **antiparallel** to, the external field.

The resonance condition is satisfied when the transition from the low to high energy states occurs and equation 13.1 is satisfied (see below). Energy must be absorbed for these transitions to occur: one quantum or  $h\nu$  (where  $h$  is the Planck

constant). In the appropriate external magnetic fields it is shown that the frequency of applied radiation,  $\nu$ , occurs in the microwave region for ESR (sometimes called **electron paramagnetic resonance** (EPR)) and the radiofrequency region for NMR (sometimes called **nuclear paramagnetic resonance**). In both techniques, two possibilities exist for determining the absorption of electromagnetic energy (at the resonance point):

- either a constant frequency is employed and the external magnetic field swept; or
- a constant external magnetic field is used and the appropriate region of the spectrum swept.

For technical reasons the more commonly employed option is the first, but the same results would be obtained if either option were chosen.

### 13.3.3 Principles

The quantum of energy required to cause the resonance condition to be satisfied, and transition between energy states in an ESR experiment, may be quantified as

$$h\nu = g\beta H \quad (13.1)$$

where  $g$  is the **spectroscopic splitting factor** (a constant),  $\beta$  is magnetic moment of the electron (termed the Bohr magneton), and  $H$  is the strength of the applied external field.

The frequency of the absorbed microwave radiation is a function of the paramagnetic species  $\beta$  and the applied magnetic field strength  $H$  (equation 13.1). This indicates that either may be varied to the same effect. The absorption of the energy is recorded as a peak in the ESR spectrum and is indicative of the presence of a paramagnetic species. The area under the peak is proportional to the concentration of that species, strictly the number of unpaired electron spins. Calibration of the instrument with known standards allows the concentration to be calculated. The standard, containing a known number of spins, must have the same line shape as the unknown for a reliable comparison to be made. Examples of standards are solutions of peroxyamine disulphonate or the solid 1,1-diphenyl-2'-picrylhydrazyl (DPHH). The solid standard contains  $1.53 \times 10^{21}$  unpaired spins per gram in the pure state and may be diluted by admixture with carbon black in order to give lower concentrations.

For a delocalised electron (some free radicals),  $g = 2.0023$  but for localised electrons, for example in transition metal atoms,  $g$  varies and its precise value gives information about the nature of the bonding in the environment of the unpaired electron within the molecule. When resonance occurs, the absorption peak is broadened owing to **spin-lattice interactions**, i.e. the interaction of the unpaired electron with the rest of the molecule. This gives further information about the structure of the molecule.

High resolution ESR may be performed by examining the hyperfine splitting of the absorption peak, which is caused by interaction of the unpaired electron with

adjacent nuclei. This yields information about the spatial location of atoms in the molecule. Proton ( $^1\text{H}$ ) hyperfine splitting for free radicals occurs in the region of 0 to  $3 \times 10^{-3}$  tesla (1 tesla =  $10^4$  gauss and is a measure of the magnetic induction, which is linearly related to the magnetic field strength) and yields data analogous to those obtained in high resolution NMR. In fact a considerable improvement in the effective resolution of an ESR spectrum may be achieved by using the **electron nuclear double resonance** (ENDOR) technique. In this approach the sample is irradiated simultaneously with microwaves for ESR and RF (radio frequency) for NMR. The RF signal is swept for a fixed point of the ESR spectrum. The output display is the ESR signal height versus swept nuclear RF. The approach is particularly useful when there is a large variety of nuclear levels that broaden the normal electron resonance line. A similar but different technique is **electron double resonance** (ELDOR), in which the sample is irradiated with two microwave frequencies. One is used for observation of the ESR signal at some point in the spectrum, whilst the other is used to sweep other parts of the spectrum. This is used to display the ESR signal as a function of the difference of the two microwave frequencies. ELDOR finds use in the separation of overlapping multiradical spectra and to study relaxation phenomena, for example chemical spin exchange.

#### 13.3.4 Instrumentation

Fig. 13.3 is a diagram of the main components of an ESR instrument. The field strengths generated by the electromagnets are of the order of 50 to 500 millitesla, and variations of less than 1 in  $10^6$  are required for highest accuracy. The monochromatic microwave radiation is produced in the Klystron oscillator, the wavelength being of the order of  $3 \times 10^{-2}$  m (9000 MHz).

The samples are required to be in the solid state; hence biological samples are usually frozen in liquid nitrogen. The first-order differential ( $dA/dH$ ) is usually plotted against  $H$ , not  $A$  versus  $H$ . Hence a plot similar to that in Fig. 12.9 is obtained and this shape is called a 'line' in ESR spectroscopy. Generally there are relatively few unpaired electrons in a molecule, resulting in fewer than 10 lines, which are not closely spaced.

#### 13.3.5 Applications

##### Metalloproteins

ESR spectroscopy is one of the main methods used to study metalloproteins, particularly those containing molybdenum (xanthine oxidase), copper (cytochrome oxidase and copper blue enzymes) and iron (cytochrome, ferredoxin). Both copper and non-haem iron, which do not absorb in the ultraviolet/visible regions, possess ESR absorption peaks in one of their oxidation states. The appearance and disappearance of their ESR signals are used to monitor their activity in the multi-enzyme systems of intact mitochondria and chloroplasts, as well as in isolated enzymes. In metalloproteins there exists a specific stereochemical structure whereby a characteristic number of ligands (frequently amino acid residues of the



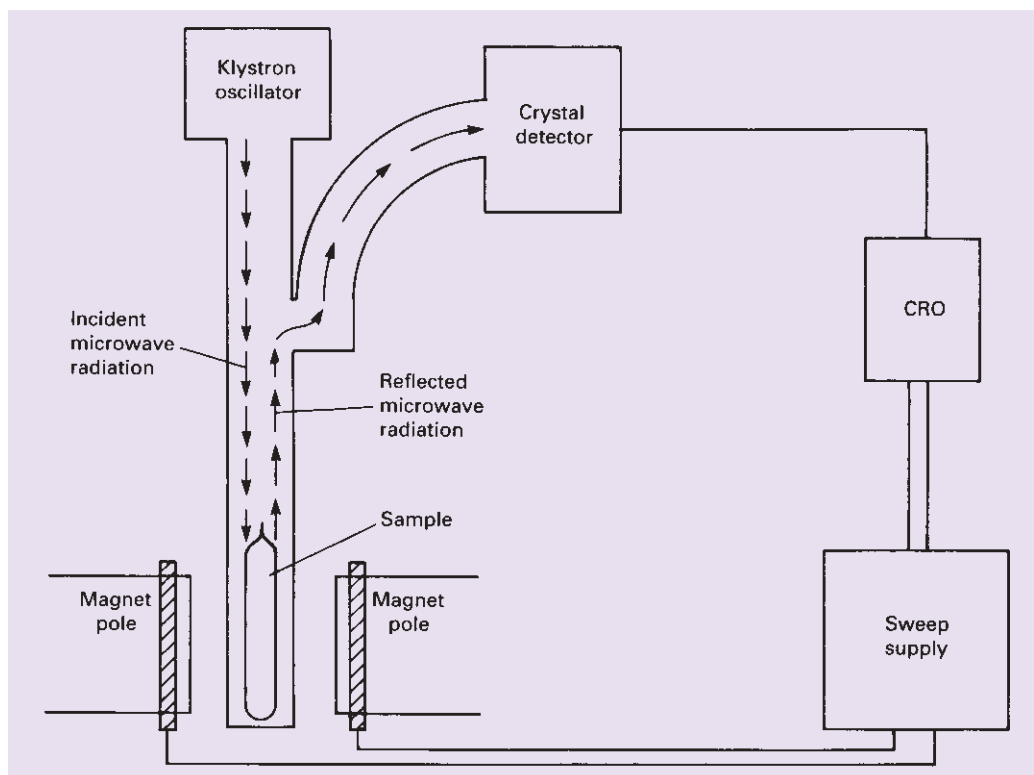


Fig. 13.3. Diagram of an ESR spectrometer. CRO, cathode ray oscilloscope.

protein) are coordinated to the metal. ESR studies show that the structural geometry is frequently distorted from that of model systems and the distortion may be related to biological function.

### Spin labels

Spin labels are stable and unreactive free radicals used as **reporter groups** or **probes**. The procedure of spin labelling is the attachment of these probes to biological molecules that lack unpaired electrons. The label can be attached to either a substrate or a ligand. Often the spin label contains the nitric oxide moiety. These labels enable the study of events that occur with a frequency of  $10^7$  to  $10^{11} \text{ s}^{-1}$ . If the motion is restricted in some directions, only **anisotropic motion** (movement in the same direction) may be studied, for example in membrane-rigid spin label in bilayers. Here the label is attached so that the NO group lies parallel to the long axis of the lipid.

Intramolecular motions and lateral diffusion of lipid through the membrane may be observed and measured. This study is achieved by either (i) concentrating the spin-labelled lipids into one region of the bilayer, or (ii) randomly incorporating, usually into model membranes. The diffusion of the spin labels allows them

to come into contact with each other and causes line broadening in the spectrum. Another label used to study lipid motion in bilayers is 2,2,6,6-tetramethylpiperidine-1-oxyl (TEMPO). Labelling of glycerophosphatides with this compound allows measurement of the flip rate between inner and outer surfaces as well as lateral diffusion.

### Free radicals

**Spin trapping** is a process whereby an unstable free radical has stability conferred upon it by reacting it with a compound such as 5,5-dimethylpyrroline-1-oxide (DMPO). Hyperfine splittings are observed that depend upon the nature of the radical R $\cdot$ .

Molecules in the triplet (phosphorescent) state (Section 12.5.1) may also be studied by ESR. This gives data complementary to that obtained in the ultra-violet/visible region of the spectrum. For instance, free radicals due to the triplet state of tryptophan have been observed in cataractous lenses.

Free radicals are found in many metabolic pathways and as degradation products of drugs and toxins. Electron transfer mechanisms in mitochondria and chloroplasts involve paramagnetic species, for example the Fe – S centres. Other redox processes involving the flavin derivatives FAD, FMN and semiquinones lend themselves readily to exploration by this approach. The  $g = 2.003$  signal is associated mainly with mitochondria, but different cell lines show different intensities. This phenomenon is also dependent on metabolic state. Factors that increase metabolic activity also lead to an increase in organic radical signal. Many studies have involved the free radical polymer melanin and the ascorbyl radical. The latter has been used to study the effects of certain drugs on sperm maturation.

Carcinogenesis is an area where free radicals have been implicated and where their study has been of value. There is, in general, a lower concentration of free radicals in tumours than in normal tissues. Also a concentration gradient is observed, being higher in the peripheral non-necrotic surface layers than in the inner regions of the tumour. The free radicals may, of course, initiate the neoplasia. The development of implanted tumours in mice has also been studied. Chemical carcinogens are in many cases associated with generation of free radicals. An example is the prediction of carcinogenicity of certain polycyclic hydrocarbons. Polycyclic hydrocarbons arise by the successive linking of benzene rings along ring edges. Examples of such compounds are naphthalene (two rings), and anthracene and phenanthrene (three rings). As more rings are added the structures become increasingly complicated. As these compounds possess 'aromatic' character it becomes increasingly possible for the free electron of the radical to be accommodated, i.e. these kinds of radicals become more stable and therefore possibly more long lived. The fact that they may survive for extended periods of time allows more damage to be done. Many of the precursors of these radicals exist in natural sources such as coal tar, tobacco smoke and other products of combustion, hence the environmental risk.

Another source of free radicals is the irradiation, for example with  $\gamma$ -rays, of biological material. For instance -S – S- cross-linkages in proteins may be identified by irradiating the protein, and the free radical produced has the free electron localised

in the -S – S-region. Another major application in this area is examining irradiated foodstuffs for residual free radicals. The technique can be used to establish whether or not the packed foodstuff has been irradiated. A similar biomedical/environmental application involves the study of hard biological materials such as bone or teeth. When such materials are exposed to ionising radiation, energy is stored in them and this energy may give rise to the production of free radicals. Clearly ESR may be used to detect these radicals and is used in 'dose assessment' in nuclear radiation accidents.

#### Metabolic studies

Many metabolic studies have made use of ESR. Examples are the metabolism of drugs, processes occurring in the microsomes of the liver, peroxidation mechanisms and the free radical products of oxygen. Superoxide dismutases scavenge oxygen-related (dioxygenyl) free radicals  $O_2^{\cdot-}$  (that have been associated, for example, with inflammation and ageing). Nitric oxide, NO, as an independent entity, operates as a physiological messenger regulating the nervous, immune and cardiovascular systems. It has been implicated in septic (toxic) shock, hypertension, stroke and neurodegenerative diseases. Although NO is involved in normal synaptic transmission, excess levels are neurotoxic. Superoxide dismutase attenuates the neurotoxicity by removal of  $O_2^{\cdot-}$ , hence limiting its availability for reaction with NO to produce peroxynitrite.

### 13.4 NUCLEAR MAGNETIC RESONANCE SPECTROSCOPY

The essential background theory of the phenomena that allow NMR to occur has been dealt with in Section 13.3.1. The miniscule magnets involved here are nucleons (in effect protons) rather than electrons. The specific principles, instrumentation and applications are treated below.

#### 13.4.1 Principles

Again there is considerable similarity with ESR. Most studies involve the use of  $^1H$  (hence the term **proton magnetic resonance** (PMR) but  $^{13}C$ ,  $^{15}N$  and  $^{31}P$  isotopes are used in biochemical studies.

The resonance condition in NMR is satisfied in an external magnetic field of several hundred millitesla, with absorptions occurring in the region of radiowave 40 MHz frequency for resonance of the  $^1H$  nucleus. The actual field scanned is small compared with the total field applied and the radio frequencies absorbed are specifically stated on such spectra.

The molecular environment of a proton governs the value of the applied external field at which the nucleus resonates. This is recorded as the **chemical shift** ( $\tau$ ) and is measured relative to an internal standard, frequently tetramethylsilane (TMS), whose structure  $(CH_3)_4Si$  contains 12 identical protons. The chemical shift arises from the applied field inducing secondary fields ( $15 \times 10^{-4}$  to  $20 \times 10^{-4}$  tesla) at the proton by interacting with the adjacent bonding electrons. If the induced field opposes the applied field, the latter will have to be at a slightly

higher value for resonance to occur. Alternatively, if the induced and applied fields are aligned the latter is required to be at a lower value for resonance. In the opposing field case, the nucleus is said to be **shielded**, the magnitude of the shielding being proportional to the electron-withdrawing power of proximal substituents. In the aligned field case, the nucleus is said to be **deshielded**. The field axis may be calibrated in units on a scale from 0 to 10, with TMS at the maximum value. The type of proton may thus be identified by the absorption peak position, i.e. its chemical shift and the area under each peak being proportional to the number of such protons in a particular group. Fig. 13.4 is a simplified diagram of an ethyl alcohol spectrum in which there are three methyl, two methylene (methene) and one alcohol group protons. The peaks appear in the area proportions 3:2:1.

High resolution NMR yields further structural information derived from the observation of **hyperfine splitting**. This arises owing to **spin-spin splitting** or **coupling**, owing to the interaction of bonding electrons with like or different spins, and may extend to nuclei four or five bonds apart. It is shown as fine-structure splitting of peaks already separated by chemical shifts. NMR spectra are of great value in elucidating chemical structures. Both qualitative and quantitative information may be obtained, and hyperfine splitting yields information about the near-neighbour environment of a nucleus. The advances in computing power have made possible many of the more advanced NMR techniques. Weak signals may be enhanced by running many scans and accumulating the data; baseline noise, which is random, then tends to cancel out whereas the real signal increases. This approach significantly improves the signal-to-noise ratio and the method is known as **computer averaging of transients** or **CAT scanning**. On combining CAT scanning with the very rapid acquisition and data processing of pulse-acquire/Fourier transform methods, very powerful tools become available. In addition the facile manipulation of data postacquisition and the generation of difference spectra has dramatically improved the usefulness and applicability of the basic technique.

Despite the value and continued use of what might be termed 'conventional' proton NMR, much more structural information may be obtained by resorting to pulsed input, of the radio frequency energy, and subjecting the resulting output to computer analysis by Fourier transform. This approach has given rise to a wide variety of procedures that allow the production of multidimensional spectra (four-dimensional in the most sophisticated experiments),  $^{13}\text{C}$  and other odd-isotope NMR spectra and the determination of multiplicities and scan images.

In common with all of the spectroscopic techniques already discussed, the energy is input in the form of electromagnetic radiation and 'entities' are promoted from lower to higher states. The 'entities' are electrons in the ultraviolet/visible techniques, bond oscillations and deformations in the infrared, Raman and microwave techniques and magnetic spin orientations in ESR and NMR. All these processes follow the strict quantum rules already described. Clearly (after a certain, albeit short, time span) the entities that were previously promoted to the higher states may return to the original condition. The general term for this process is **relaxation**. A very simple example is observable in the ultraviolet/visible region,

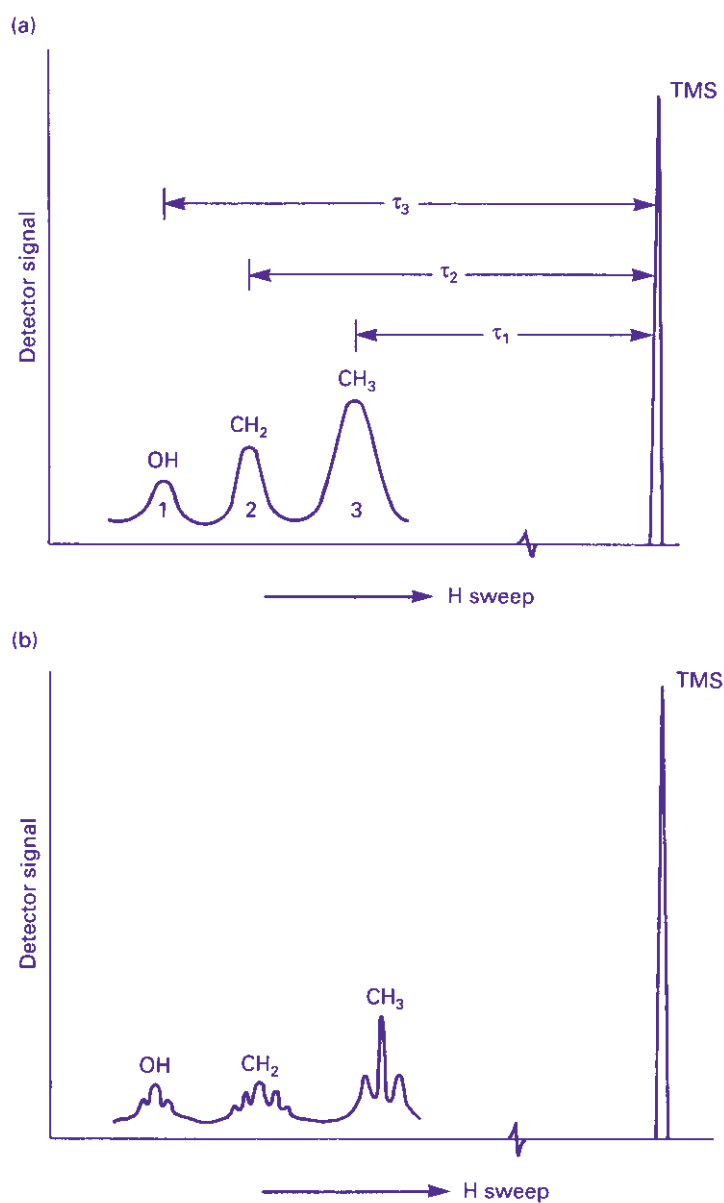


Fig. 13.4. NMR spectrum of ethyl alcohol (a) at low resolution and (b) at high resolution. The latter resolved only in very pure samples. TMS, trimethylsilane.

where an absorption spectrum arises when the energy is input and absorbed and an emission spectrum when the system relaxes.

#### Pulse-acquire and Fourier transform methods

A number of approaches to the method used for the production of spectra exists but mainly one of two options is used. In 'conventional' spectroscopy the electromagnetic energy is supplied, from the source, as a continuously changing

frequency over a preselected spectral range. The response is detected by an appropriate device and whether the *scan* is from shorter to longer wavelength (higher to lower frequency), or the reverse, is irrelevant. The essential point is that the change is smooth and regular between fixed limits. The alternative is to put all the energy, i.e. all the resonant frequencies between the fixed limits, in at the same time. This is achieved by irradiating the sample with a broadband pulse of all these frequencies at one go. The output is, of course, also measured simultaneously and the observed result is, in general, a very complicated interference pattern. Fortunately these patterns are amenable to analysis by Fourier transform methods, which, although being quite complicated mathematical procedures, can be performed readily using modern computer facilities and appear transparent to the user.

The approaches differ with the spectroscopic technique. As indicated in Section 13.2.2, FT-IR involves the method of *interferometry* and the *interferograph* that results arises from observation of the frequencies which pass through the sample and are not absorbed. What is detected in FT-NMR is known as the *free induction decay* (FID). This is akin to the emission spectrum referred to in ultra-violet/visible methods in that the FID arises from the excited species re-emitting the absorbed frequencies. The discussion so far has, for the sake of simplicity, attempted to describe the observed phenomena in terms of single entities, i.e. single nuclei. In a real sample of material in which bulk magnetism may be observed, this arises from the accumulation of all the miniscule nuclear magnets. It may be demonstrated using Boltzmann statistics that, when the sample is placed in an external magnetic field, at thermal equilibrium there will be a slight excess of spins, the so-called  $\alpha$ -spins, aligned or parallel with this field. Note that this is the normal low energy condition, the high energy state being that of the *antiparallel*  $\beta$ -spins. This gives rise to the bulk magnetisation vector,  $\mathbf{M}$ , and, by agreed convention, it is taken to lie along the z-axis of a three-dimensional Cartesian coordinate system, the z-axis being parallel to the direction of the external magnetic field. The magnetic induction of the external field is designated  $B_0$ . Now consider the input of a pulse of the appropriate radio frequency (RF) radiation. Recall that this is electromagnetic radiation comprising an electric and a magnetic vector. The magnetic vector of the RF radiation has an associated magnetic field whose magnetic induction may be designated  $B_1$ . If the transmitter coils supplying the pulse of RF radiation are arranged so that  $B_1$  is perpendicular to the z-axis along which the bulk magnetisation vector,  $\mathbf{M}$ , lies, then  $\mathbf{M}$  will be rotated through an angle  $\theta$  towards the  $x$ - $y$  plane. The value of  $\theta$  depends upon the magnitude of the  $B_1$  field and the duration of the pulse. Fig. 13.5a,b is a diagrammatic representation of this process, with  $\theta = \pi/2$  for simplicity (see 'Multidimensional NMR', below, for further explanation). The cumulative spins comprising  $\mathbf{M}$  are no longer parallel to the external magnetic field, i.e.  $\mathbf{M}$  no longer lies along the z-axis. In the absence of a further pulse of RF radiation the system will relax,  $\mathbf{M}$  returning to lie along the z-axis. It is this return or relaxation, which is first-order exponential, that gives rise to the free induction decay alluded to above and data are acquired during the decay period. As described, this would be known as a simple *pulse-acquire experiment*. *Multipulse RF input*, possibly at different angles, gives rise to a large array of

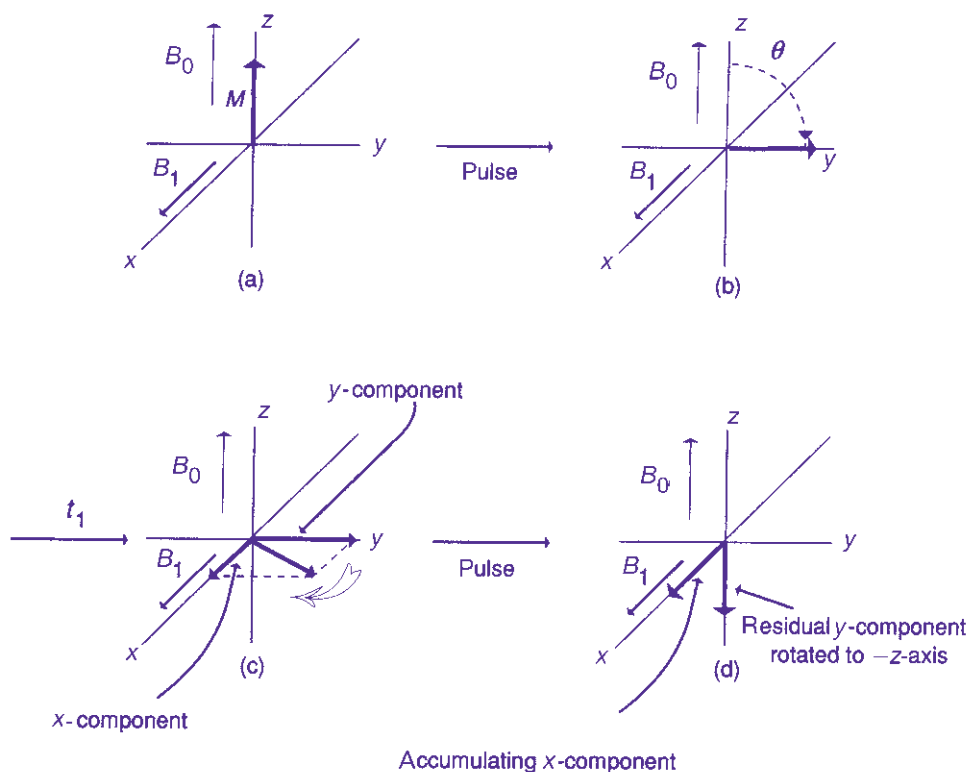


Fig. 13.5. Rotation of magnetism during radio frequency pulses.

different experiments, resulting in the production of extremely valuable data. Two relaxation processes are important in NMR and associated techniques. The first-order exponential decay observed in FID arises from energy dissipation by spin–lattice or longitudinal relaxation. In this situation the energy is lost to the matrix (surroundings). The time span for this process is designated  $T_1$ . An alternative process is spin–spin or transverse relaxation with time span  $T_2$ , where energy is dissipated between spins rather than the environment.  $T_1$  is always greater than or equal to  $T_2$  and for small organic molecules they are equal.

It is beyond the scope of this text to examine the specific details of the Fourier transform method. It is sufficient to recognise that the mathematical procedure effects the translation of a signal in the time domain to a corresponding ‘peak’ in the frequency domain. For a sine wave of single frequency,  $\nu$  Hz (cycles per second), 1 cycle is mapped in  $1/\nu$  seconds. The ordinary sine wave is normally shown in the time domain as a portion of an infinite cycle of oscillations of constant amplitude. The frequency appears as a single peak in the frequency domain, also of fixed amplitude. Fig. 13.6a shows the effect of the translation between domains for a single sine wave and Fig. 13.6b that for the single FID pattern. All complicated interference patterns may be separated into their constituent sine and cosine waves by Fourier analysis and transformed between domains. Fig. 13.7

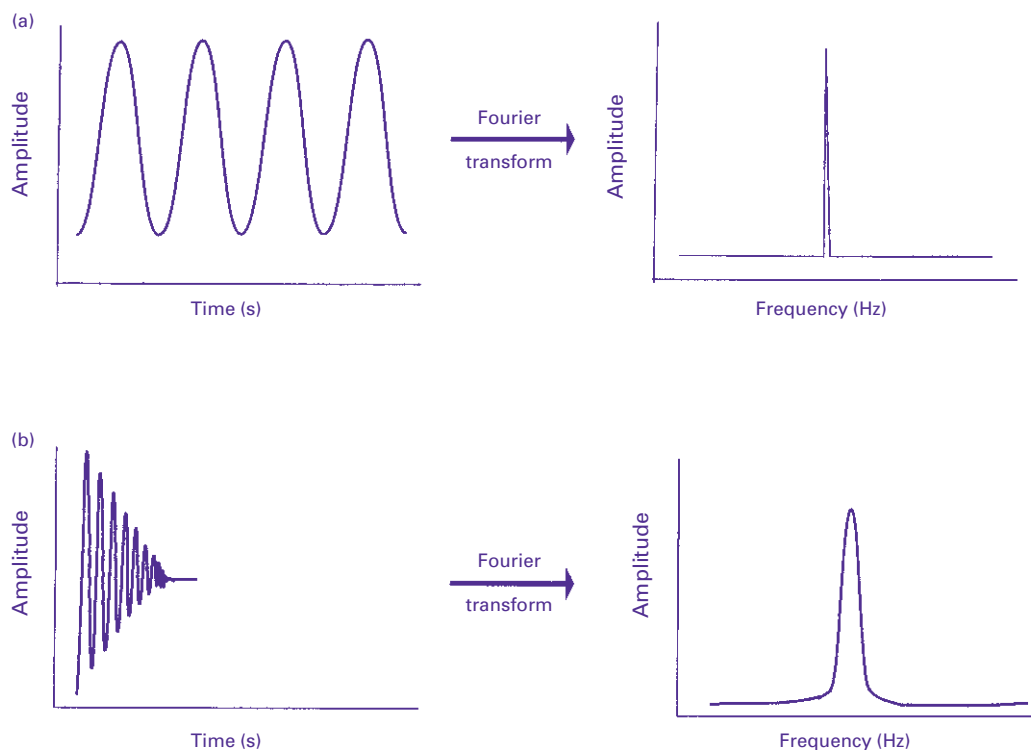


Fig. 13.6. Diagrammatic representation of the Fourier transformation of a single frequency sine wave and single FID. (a) Sine wave, (b) single free induction decay.

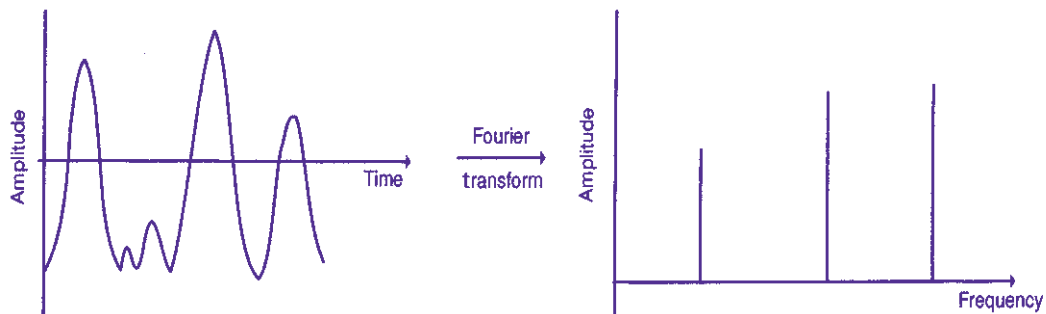


Fig. 13.7. FT of a three-sine-wave combination.

shows the transform of a waveform comprising three sine waves of different frequency and amplitude.

The time domain oscillograph representing the FID from a real NMR experiment would of course be much more complicated, as it would comprise many more contributory sine and cosine waves. These would be extracted, transformed to the frequency domain and presented as peaks in a spectrum.



In Section 13.3.2 it was indicated that spins or spinning nuclei generate magnetic fields that may extend their influence through space. Proximal neighbours are subject to this influence, directly, and the general term for this phenomenon is dipolar interaction. If the signal intensity of a resonance is observed to change when the state of a near neighbour is perturbed from the equilibrium, then what is being seen is an example of the **nuclear Overhauser effect** (NOE). This effect is of profound importance in the elucidation of the three-dimensional stereochemistry of the molecular species under investigation. The magnetic influences encountered in the dipolar interaction are transmitted through space over a limited distance and for the NOE to be observed the distance between nuclei must be of the order of about 0.4 nm or less. Clearly this spatial constraint enables information to be gained about the three-dimensional geometry of the molecule being examined when considered together with scalar coupling (spin–spin coupling) information, this being the influence whose effects occur through bonds.

It is possible to saturate spins in a given population (the perturbation) with a selective 90° irradiation, giving ample time for the acquisition of proton spectra involving <sup>1</sup>H–<sup>1</sup>H interactions giving rise to NOE enhancements. By performing a second irradiation at a point in the RF spectrum that is remote from any resonant frequencies, **off-resonance irradiation**, a control spectrum (no NOEs produced) is generated that may be subtracted from the previously acquired one, resulting in the cancelling out of any signals that are not NOE enhancements. The results obtained are referred to as **steady-state NOEs** and the method is termed the **NOE difference experiment**.

One of the main advantages to be gained from the use of pulse-acquire/Fourier transform methods coupled to signal averaging, together with the development of high field magnets, is the ability to obtain <sup>13</sup>C NMR spectra. This isotope of carbon exists in low abundance, 1.108%, and compared to the essentially 100% abundance of <sup>1</sup>H it may be recognised that, in general, signal intensities are likely to be low. Despite the advances described above, about 10 times the amount of sample, in most cases, is required for <sup>13</sup>C NMR spectra as compared with that for <sup>1</sup>H spectra.

Owing to the low abundance of the <sup>13</sup>C nucleus, the chance of finding two such species next to each other in a molecule is very small. This is considered in more detail in Chapter 9. In consequence of this, <sup>13</sup>C–<sup>13</sup>C interactions (**homonuclear couplings**) do not arise. It is true that <sup>1</sup>H–<sup>13</sup>C interaction (**heteronuclear coupling**) is possible but, for technical reasons such as band overlap, it is usual to generate **decoupled spectra**. The result is that, in general, <sup>13</sup>C spectra are very much simpler and cleaner and have improved signal-to-noise ratios (albeit with higher sample loadings) compared with their proton resonance counterparts. There are clear advantages in this approach but at least one considerable disadvantage. The ability to observe multiplicities has been lost, i.e. whether a particular <sup>13</sup>C is associated with a methyl (CH<sub>3</sub>), methene (CH<sub>2</sub>) or methyne (CH) group. Some of this information may be regained by performing the decoupling using off-resonance irradiation as in the NOE difference experiments described above. However, a method that has become routine is **distortionless enhancement by polarisation transfer** (DEPT). This method requires a multipulse excitation sequence at different angles,

frequently  $45^\circ$ ,  $90^\circ$  or  $135^\circ$ . Although interactions have been decoupled, in this situation the resonances exhibit positive or negative signal intensities, or signal phases, which are dependent on the number of protons directly attached to the carbon nucleus. For example, in a DEPT-135 experiment: CH and CH<sub>3</sub> are both positive; CH<sub>2</sub> is negative. Clearly a single DEPT-135 experiment would suffice if no methyl groups are present. DEPT signals for the above primary, secondary or tertiary carbons, from irradiations at  $45^\circ$  and  $90^\circ$ , are either positive or zero.

### Multidimensional NMR

Consider further the processes described in Fig. 13.5a–d. The magnetisation vector  $\mathbf{M}$  is originally aligned along the  $z$ -axis parallel to the vector direction of the external field,  $B_0$ . A pulse  $B_1$  is applied, at right angles, i.e. parallel to the  $x$ -axis and  $\mathbf{M}$  is rotated to the  $y$ -axis through  $90^\circ$ , provided the pulse is of sufficient magnitude and lasts for a sufficient time (Fig. 13.5a,b). Apart from the decay process this vector will precess (rotate) in the  $x$ – $y$  plane, towards the  $x$ -axis (Fig. 13.5c) with a characteristic frequency, the **Larmor frequency**, during a period of time  $t_1$ . This is quite distinct from the decay process, FID, which overlaps it. At any point between the  $x$ - and  $y$ -axes the vector  $\mathbf{M}$  may be resolved into components along these two axes. If, during  $t_1$ , a second  $B_1$  pulse is applied then the component along the  $y$ -axis will again be rotated, in this instance towards the  $-z$ -axis. The component along the  $x$ -axis is unaffected because it is parallel to  $B_1$ . If the time  $t_1$  is zero, i.e. there are immediately consecutive  $B_1$  pulses, then  $\mathbf{M}$  rotates from the  $z$ - to the  $y$ -axis with the first pulse and then immediately to the  $-z$ -axis with the second pulse. For  $t_1 = 0$  there will be no  $x$  component as there has been no time available for it to be established. For values of  $t_1 > 0$  a component of  $\mathbf{M}$  along the  $x$ -axis will be established whose magnitude depends on the length of  $t_1$ . The longer  $t_1$  the greater will be the magnitude of the  $x$  component because  $\mathbf{M}$  will have moved nearer to this axis. By applying successive  $B_1$  pulses with increasing lengths of  $t_1$ , an accumulated  $x$  component of magnetisation is produced and a series of FIDs may be measured and stored separately in the computer. The  $y$ - and  $-z$ -components are not measurable. This accumulation of FIDs gives rise to a second dimension in the time domain and each may be transformed by Fourier methods.

Two-dimensional frequency diagrams are produced as contour maps. Values on the diagonal correspond to chemical shifts, etc., that would have been shown in a one-dimensional experiment. It is the asymmetrical, off-diagonal information that is new. These data arise from the correlation of coupling interactions between nuclei, the main advantage being that the information is all gathered in one experiment, an achievement entirely dependent on the use of multipulse excitation. Proton–proton correlation gives rise to **homonuclear correlation spectroscopy** (COSY). Proton–carbon correlation gives rise to **heteronuclear chemical shift correlation spectroscopy** (hetero-COSY or HETCOR).

The achieved and potential sophistication of NMR experiments is quite phenomenal, allowing more useful two-dimensional and extension into three- and four-dimensional spectra. Considering again Fig. 13.5a–d (the COSY pulse

sequence), the second  $90^\circ$  pulse rotates the magnetisation vector along the  $-z$ -axis. Various transverse components are removed by electronic control and the vector in the  $-z$  direction accumulates (cf. the process described above for the COSY case). A third  $90^\circ$  pulse is then applied and produces magnetisation, which can be measured. Repeat of the pulse sequence for varying (increasing) values of  $t_1$  gives rise to changes that are observable during the final  $90^\circ$  pulse. The outcome is a two-dimensional experiment that allows the detection of NOEs and is known as **nuclear Overhauser effect spectroscopy** (NOESY). This can be improved upon yet further by studying phenomena in the rotating frame coordinate system rather than fixed Cartesian coordinates. Such an experiment involves **rotating frame nuclear Overhauser effect spectroscopy** (ROESY). A significant problem is that, for  $^1\text{H}$  NOESY NMR to be of value, all the NOEs should be resolved. In the study of biological macromolecules this becomes less likely with the increase in molecular mass. The use of triple pulse sequences (three time variables) in conjunction with a COSY or NOESY sequence generates a three-dimensional spectrum. This, in effect, is a cube and is akin to stacking two-dimensional spectra one on top of the other. Note that this is a near analogy and not a simple stacking procedure. In order to achieve this it is necessary to incorporate into the molecule under investigation an isotopically labelled nuclide such as  $^{13}\text{C}$  or  $^{15}\text{N}$ . A whole new range of interactions between  $^1\text{H}$ ,  $^{13}\text{C}$  and/or  $^{15}\text{N}$  is now possible and adds extensively to the analytical procedure. To obtain the resolution advantages of the four-dimensional spectrum, both  $^{13}\text{C}$  and  $^{15}\text{N}$  must be incorporated, the heavy isotope of carbon being deliberately introduced at particular points in the carbon chain in order to be associated with specific aliphatic hydrogens. Essentially, three separate two-dimensional experiments are combined, the different interactions being  $^1\text{H}$ - $^1\text{H}$ ,  $^1\text{H}$ - $^{13}\text{C}$  and  $^1\text{H}$ - $^{15}\text{N}$ . It is interesting to note that, in the four-dimensional case, the manipulation of the generated data by powerful computer techniques results in substantially improved resolution without a corresponding increase in complexity.

#### 13.4.2 Instrumentation

The essential details of an NMR instrument are shown diagrammatically in Fig. 13.8. It will be seen yet again that the layout is almost identical to that of ESR, except that instead of a Klystron oscillator being present to generate microwave radiation, two sets of coils, a transmitter and a receiver, are used for generation and reception, respectively, of the appropriate RF. Samples in solution are contained in sealed tubes, which are rotated rapidly in the cavity to eliminate irregularities and imperfections; in this way an average and uniform signal is reflected to the receiver to be processed and recorded. Solid state and high field NMR are more recent and rapidly advancing techniques enable hitherto difficult or impossible investigations. The latest developments allow multidimensional NMR to be performed, permitting even more sophisticated structural analyses to be carried out. Many of these developments in instrumentation differ from the simple design shown in Fig. 13.8 in terms of the geometric layout of the coils, for the multipulse methods described above, sophisticated electronics and advanced computer facilities.

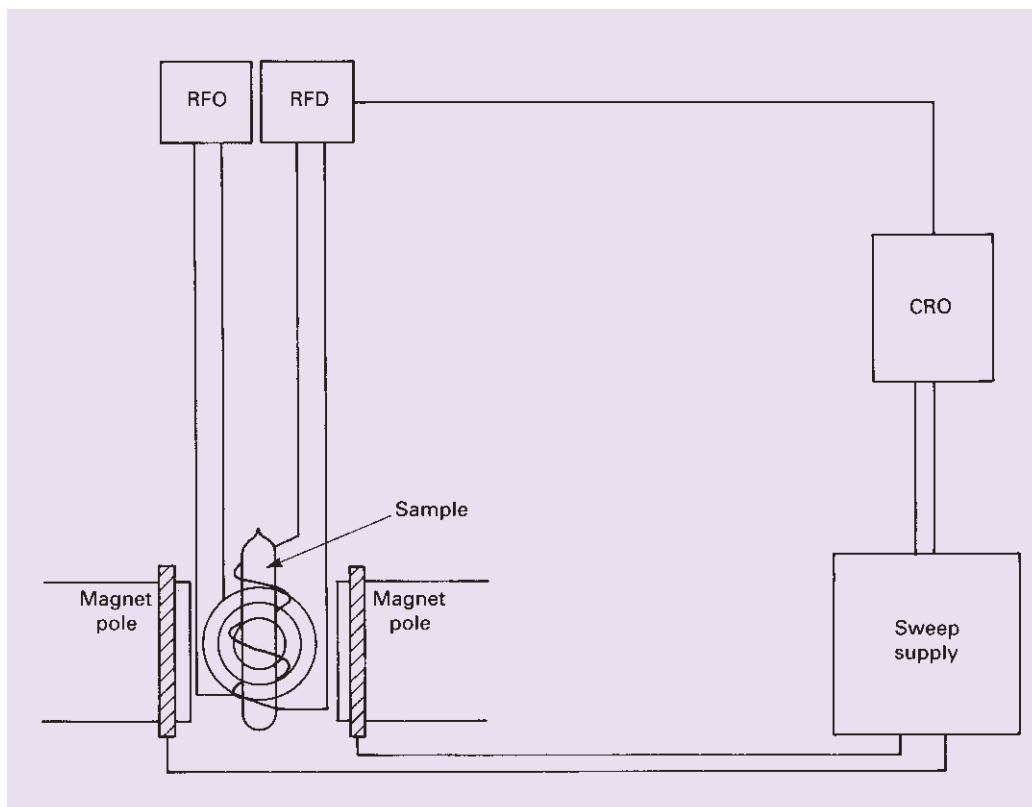


Fig. 13.8. Diagram of an NMR spectrometer. CRO, cathode ray oscilloscope; RFO, radio frequency oscillator; RFD, radio frequency detector.

### 13.4.3 Applications

#### Molecular structure determination

The study of molecular structure, conformational changes and certain types of kinetic investigation is the main use of NMR in the biological field. Most work is done in solution, and in order to eliminate solvent effects the equivalent deuterated solvent (for proton NMR) would be used. The use of the technique in drug metabolism studies is of increasing importance, particularly when coupled with infrared and X-ray diffraction data, which can then be used in molecular modelling methods using sophisticated computer techniques to try to elucidate drug action. Fig. 13.9 shows a high resolution proton resonance spectrum of phenacetin and, together with the FT-IR spectrum shown in Fig. 13.2, yields substantial structural information. For comparative purposes, the two-dimensional COSY spectrum of phenacetin is shown in Fig. 13.10, where contours along the diagonal give information equivalent to that shown in Fig. 13.9. The off-diagonal contours represent additional information; for explanation, see the legend to Fig. 13.10.

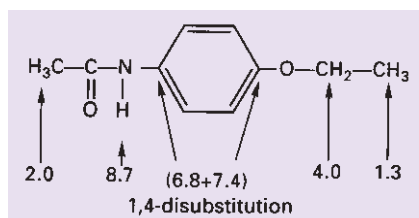
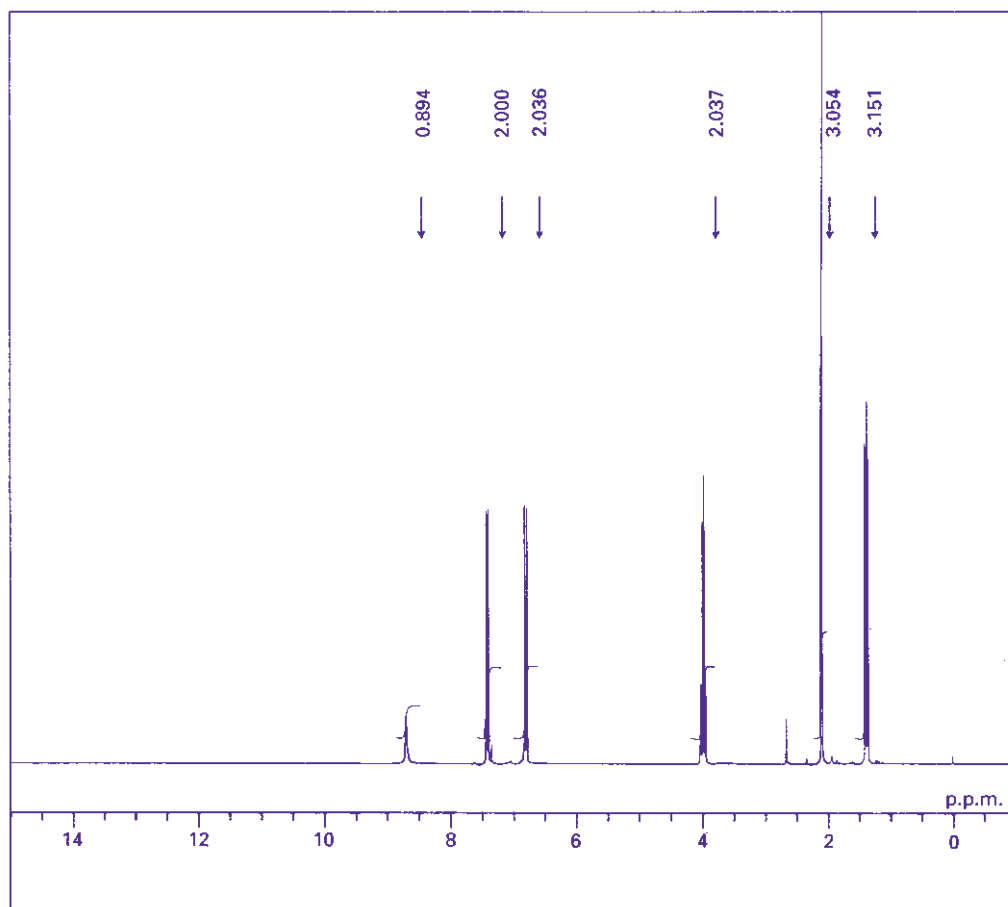
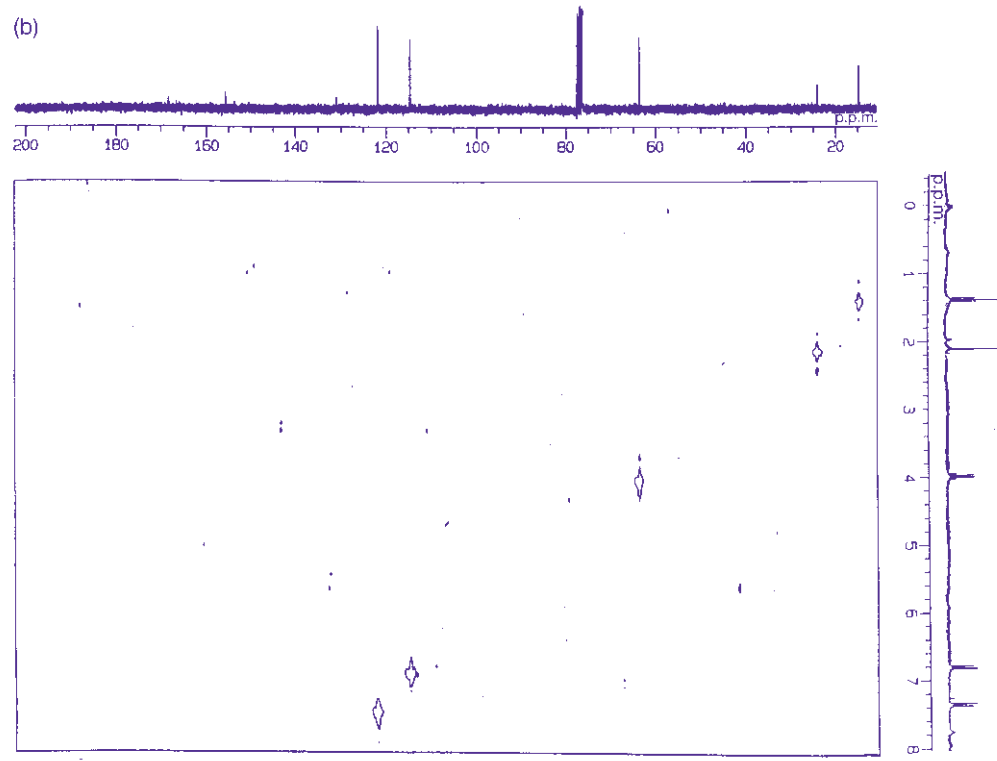
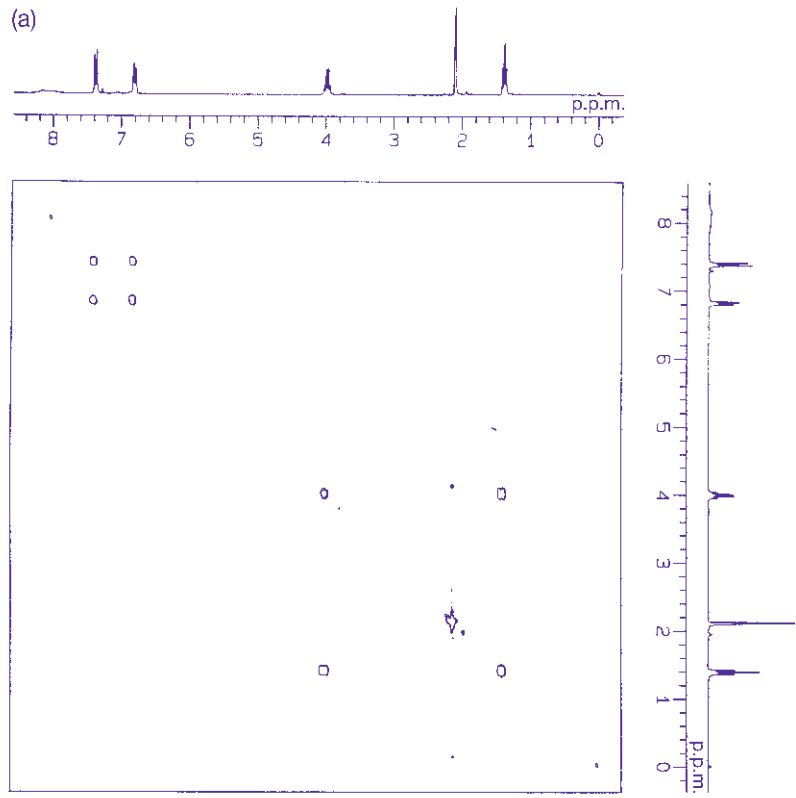


Fig. 13.9. NMR spectrum of phenacetin. The values associated with the downward-pointing arrows, shown slightly to the right of each peak in the upper diagram, indicate the approximate number of protons involved. In the lower diagram the shifts in p.p.m. are shown, indicating which proton is involved. The peak at 1.3 p.p.m. is a triplet because it is next to a  $\text{-CH}_2$  group and that at 4.0 is a quadruplet because it is next to a  $\text{-CH}_3$  group. The peaks at 6.8 and 7.4 p.p.m. are a pattern characteristic of 1,4 disubstitution in an aromatic ring.



An examination of the scientific literature in the field shows a plethora of results for biological macromolecules using the whole battery of techniques described above. For peptide and protein structural studies the species tend to be arbitrarily divided into those with relative molecular mass less than 15 000 and those between 15 000 and 30 000. Low resolution NMR has been obtained on the *lac* repressor headpiece and bovine pancreatic trypsin inhibitor (BPTI). High resolution protein structures for antiviral protein BDS-1, the C3a and C5a inflammatory proteins, plastocyanin, thioredoxin, epidermal growth factor and the interleukins are some examples. The application of solid state NMR has been valuable in the study of, for example, Alzheimer's  $\beta$ -amyloid peptide and melatonin. Much more specialised methods are required to extend the mass range beyond 30 000 but it is now possible and several antibodies have been investigated.

### Structures in aqueous solution

A distinct advantage of NMR is its use in studying molecular behaviour in solution. Any particular state is averaged, of course, but often produces more useful

**Fig. 13.10.** Two-dimensional NMR spectra may be best imagined as looking down on a forest where all the trees (representing peaks in the spectrum) have been chopped off at the same fixed height. Taller trees would have thicker trunks at a given height. The equivalent is the larger contours observed which derive from larger peaks in the unidimensional spectra.

(a) This figure is the correlated (COSY) NMR spectrum of phenacetin showing the homonuclear  $^1\text{H}-^1\text{H}$  interactions. The single spectra along each axis are identical and the contours along the diagonal of the two-dimensional map represent the 'birds-eye view' of the chopped-off peaks. The off-diagonal contours, which are symmetrically distributed as a mirror image about the diagonal, represent new information. As an example of the interpretation, place a rule horizontally at the 1.3 p.p.m. position of the right-hand spectrum (triplet) and another rule vertically at the 4.0 p.p.m. position on the top spectrum (quadruplet). Where these two rules intersect is the location of a contour which represents the interaction between protons located in adjacent  $-\text{CH}_2-$  and  $-\text{CH}_3$  groups.

(b) This is the heteronuclear  $^{13}\text{C}-^1\text{H}$  correlation spectrum. The contours in the two-dimensional map here represent interactions between the nuclear magnets of  $^{13}\text{C}$  and the associated protons. The  $^1\text{H}$  spectrum lies vertically along the right-hand axis and the  $^{13}\text{C}$  spectrum lies horizontally along the top. The contour positions are located as described in (a) above and the p.p.m. values and interactions are listed below.

p.p.m.		
$^{13}\text{C}$	$^1\text{H}$	Interaction
14	1.3	$\text{CH}_3-$ (Ethyl-O)
24	2.1	$\text{CH}_3-$ (Acetyl)
63	4.0	$\text{CH}_2-$ Ethyl-O)
115	6.8	Ring C (Ethyl-O)
122	7.4	Ring C (= N-H)
132	—	Ring C (= N-H)
156	—	Ring C (Ethyl-O)
167	—	= C = O
	7.8	= N - H

A triplet observed at 77 p.p.m. is due to residual chloroform in the solvent.

information than the constrained structures available from X-ray crystallographic studies. Results of studies of protein folding are exemplified by ribonuclease A, cytochrome *c*, barnase,  $\alpha$ -lactalbumin, lysozyme, ubiquitin and BPTI.

The techniques have been applied to the study of enzyme kinetics both *in vivo* and *in vitro*. Amongst the groups of enzymes studied are: chymotrypsin, trypsin, papain, pepsin, thermolysin; adenylate, creatinine and pyruvate kinases; alkaline phosphatase, ATPase and ribonuclease (Section 15.4.7). Other examples are glycogen phosphorylase, dihydrofolate reductase and triosephosphate isomerase.

### Nucleic acids

Application to the nucleic acids includes not only a variety of structural studies of both DNA and RNA but additionally investigations of interactions between various drugs and DNA and between binding proteins and DNA. Sequence assignments in oligosaccharides have been obtained but work on intact glycoproteins has not been promising, particularly in multidimensional NMR, owing to the difficulty in deconvoluting the data. Interactions between proteins and lipid bilayers in membranes have been observed and the structure of certain membrane proteins has been related to their predicted biological function. Examples of such proteins are gramicidin A, bacteriorhodopsin and rhodopsin, phage coat proteins and alamethicin.

### Phosphate metabolism

The isotope  $^{31}\text{P}$  exhibits nuclear resonance and NMR has been used extensively in studies of phosphate metabolism. The relative and changing concentrations of AMP, ADP and ATP can be measured and hence their metabolism studied in living cells and tissues. Intracellular and extracellular inorganic phosphate concentrations may be measured in living cells and tissues also because the chemical shift of inorganic phosphate varies with pH.

### Magnetic resonance imaging

The analytical applications described above may be extended into the clinical environment. Physiological material such as urine, blood and cerebrospinal fluid may be studied directly. Appropriate tissue biopsy samples are also amenable to examination. In such cases, biochemical phenomena are being observed. For instance, the measurement of metabolic concentrations at specific sites in tissues is possible. The extension to small whole animals in pharmacological investigations and the human subject has become possible with the advent of superconducting magnet technology and other improvements. ATP metabolism in healthy and unhealthy individuals and changes during exercise are measurable.

The major direct clinical application, however, is in **imaging**. Unfortunately, owing to the low energy transitions in the radio frequency region of the electromagnetic spectrum, NMR is a relatively insensitive technique. This imposes limitations and attention is focused almost exclusively on  $^1\text{H}$  resonance in the development of magnetic resonance imaging (MRI). There are two important reasons for this:



first the proton is one of the more sensitive nuclides, and, secondly, it is present in biological systems in considerable abundance. However, not all types of proton in all molecular environments are easily studied. Those protons making a major contribution to the NMR response reside in compounds in rapid physical motion. By far the most important compound in this respect is water, which contains two protons and is a major constituent of biological systems. Lesser contributions from protons in other compounds are measurable in special circumstances.

In NMR, the resonance frequency of the particular nuclide contributing the magnetic spin is proportional to the strength of the applied external magnetic field. If an external magnetic field 'gradient' is applied then a range of resonant frequencies may be observed which reflects the spatial distribution of the spinning nuclei. Three major approaches are in wide use which result in (i) projection reconstruction, (ii) Fourier imaging and (iii) echo-planar imaging. For detailed consideration of these different methods the reader is referred to more specialised texts (see Section 13.5).

A particular advantage of MRI is that there is some flexibility in the choice of physical property that is imaged. The number of spins in a particular, defined spatial region gives rise to the spin density as a measurable parameter. This measure may be combined with measures of the principal relaxation times ( $T_1$  and  $T_2$ ) to give more meaningful results. The imaging of flux, as either bulk flow or localised diffusion, adds considerably to the options available. In terms of whole-body scanners the 'overall picture' is reconstructed from images generated in contiguous slices and clearly owes much to advances in computing power as well as magnetic resonance technology. Resolution and image contrast are major considerations for the technique and subject to continuing development. Equipment cost and data acquisition time remain other important issues affecting the development of MRI.

Water is distributed differently in different tissues but constitutes, in total, about 55% of body mass in the average human subject. In soft tissues the water distribution varies between 60% and 90% of the total mass. The differences in water content in white and grey matter in the brain and between normal tissue and most tumours generate sufficient contrast to enable high resolution images to be produced. Fig. 13.11 reproduces an MRI scan showing a vertical longitudinal section of the human head and brain. In adipose tissue the  $^1\text{H}$  signal from lipids is measurable and the chemical shift differences for  $-\text{CH}_2-$  are such that distinction from water may be made. Reproduced in Fig. 13.12 are photographs obtained from MRI scans of fat and thin patients in order that the distribution of adipose tissue may be compared. The thin patient represents the control in the experiment.

It is also possible to distinguish the different relaxation properties. Tissue water behaves quite differently from the pure substance. Transverse relaxation,  $T_2$ , does not generally follow a single exponential decay process whereas longitudinal relaxation,  $T_1$ , does.  $T_2$  relaxations must be split into at least two exponential decays, having a typical value of 20–100 ms. For  $T_1$  decays the range is 100–500 ms. These values are significantly less than for pure water and the differences may

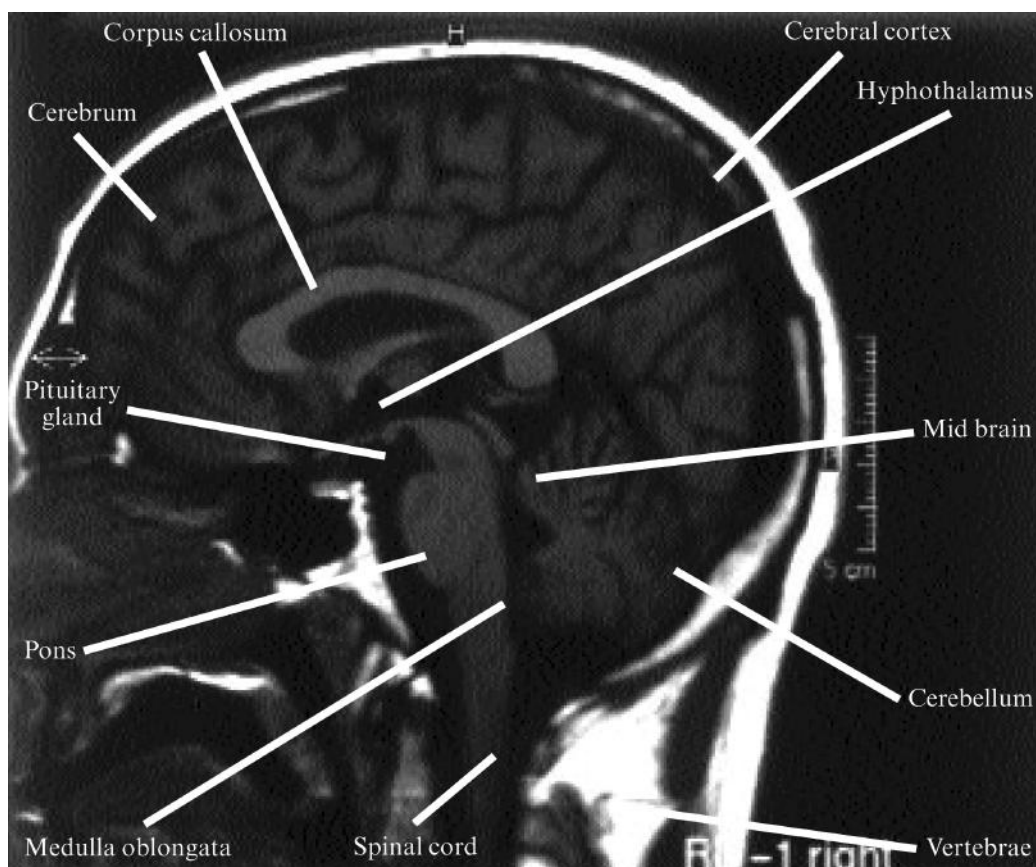


Fig. 13.11. Vertical longitudinal section through the human head by magnetic resonance imaging (MRI). The major features are identified and labelled, although specific items such as the pituitary gland and hypothalamus are barely visible. (This figure is modified from an MRI scan kindly donated by the Radiology Department of the Stepping Hill Hospital, Stockport, Cheshire.)

arise from the presence of hydrophilic macromolecules in the tissue environment. In the case of tumours, however, the  $T_1$  values are elevated compared with normal tissue, adding a further important discriminator, although the elevation is less marked in human tumours compared with laboratory-grown material. Disadvantages with this approach are the overlap of values and also that elevated  $T_1$  decays are not tumour specific but may also be evident in normal rapidly regenerating tissue. Other NMR parameters and observational differential diagnosis of the magnetic resonance image must also be taken into account. The shape, size and location of the abnormal image must be considered by the radiologist when making a diagnosis.

At present there is an almost bewildering array of options available in terms of different pulse sequences, scan protocols, and chemical shift and relaxation time data measurements that can be made. The procedures can be applied to

(a)



Fig. 13.12. (a) and (b) show MRI scans of transverse sections (contiguous slice) through the abdominal regions of 'fat' and 'obese' subjects. The fatty deposits are indicated by the intense white regions, the resonance arising from the protons of the methylene groups of long-chain fatty acids. (The scans are reproduced by kind permission of the Oxford Lipid Metabolism Group, Nuffield Department of Clinical Medicine, University of Oxford.)

three-dimensional and contiguous slice imaging of whole body or specific organ investigations on head, thorax, abdomen, liver, pancreas, kidney and musculo-skeletal regions. Use of contrast agents has enabled 'organ function' such as renal function to be explored, if the agent passes into the urine. If such an agent can be administered intravenously then exploration of blood flow, tissue perfusion, and transport across the blood/brain barrier may be investigated and also defects in vascular anatomy recognised. Contrast agents for use in MRI will generally be required to show paramagnetic properties. Clearly, as in other invasive methods, they must be non-toxic.

NMR and the associated technique of MRI offer the analytical biochemist and the clinician a phenomenal variety of procedures. Both types of application continue to challenge almost all alternative approaches. Clearly there are hazards associated with any technique but these magnetic resonance methods appear, on the basis of current knowledge, to be relatively safe, particularly with the absence of ionising radiation.

(b)

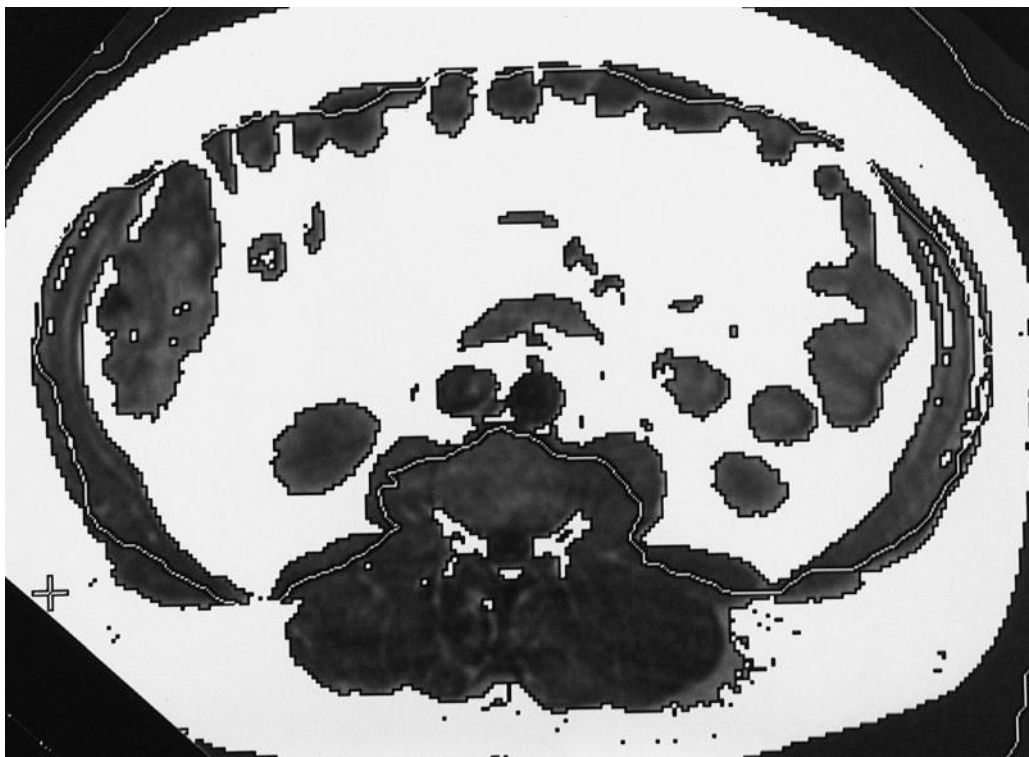


Fig. 13.12. (Cont.)

### 13.5 SUGGESTIONS FOR FURTHER READING

EVANS, J. N. S. (1995). *Biomolecular NMR Spectroscopy*. Oxford University Press, Oxford.

(Contains several excellent chapters on the application of NMR to the study of enzymes.)

REID, D. G. (1997). *Protein NMR Techniques*. Humana Press, Totawa, NJ. (Includes some good

examples of the application of single and multidimensional NMR to the study of proteins.)

## Radioisotope techniques

### 14.1 THE NATURE OF RADIOACTIVITY

#### 14.1.1 Atomic structure

An atom is composed of a positively charged nucleus that is surrounded by a cloud of negatively charged electrons. The mass of an atom is concentrated in the nucleus, even though it accounts for only a small fraction of the total size of the atom. Atomic nuclei are composed of two major particles, **protons** and **neutrons**. Protons are positively charged particles with a mass approximately 1850 times greater than that of an orbital electron. The number of orbital electrons in an atom must be equal to the number of protons present in the nucleus, since the atom as a whole is electrically neutral. This number is known as the **atomic number** ( $Z$ ). Neutrons are uncharged particles with a mass approximately equal to that of a proton. The sum of protons and neutrons in a given nucleus is the **mass number** ( $A$ ). Thus

$$A = Z + N$$

where  $N$  is the number of neutrons present.

Since the number of neutrons in a nucleus is not related to the atomic number, it does not affect the chemical properties of the atom. Atoms of a given element may not necessarily contain the same number of neutrons. Atoms of a given element with different mass numbers (i.e. different numbers of neutrons) are called **isotopes**. Symbolically, a specific nuclear species is represented by a subscript number for the atomic number, and a superscript number for the mass number, followed by the symbol of the element. For example:



However, in practice it is more conventional just to cite the mass number (e.g.  ${}^{14}\text{C}$ ). The number of isotopes of a given element varies: there are 3 isotopes of hydrogen,  ${}^1\text{H}$ ,  ${}^2\text{H}$  and  ${}^3\text{H}$ , 7 of carbon  ${}^{10}\text{C}$  to  ${}^{16}\text{C}$  inclusive, and 20 or more of some of the elements of high atomic number.

#### 14.1.2 Atomic stability and radiation

In general, the ratio of neutrons to protons in the nucleus will determine whether an isotope of a given element is stable enough to exist in nature. **Stable isotopes** for

**Table 14.1** Properties of different types of radiation

Alpha	Beta	Gamma, X-rays and Bremmstrahlung
Heavy charged particle	Light charged particle	Electromagnetic radiation (em)
More toxic than other forms of radiation	Toxicity same as em radiation per unit of energy	Toxicity same as beta radiation per unit of energy
Not penetrating	Penetration varies with source	Highly penetrating

elements with low atomic numbers tend to have an equal number of neutrons and protons, whereas stability for elements of higher atomic numbers is associated with a neutron:proton ratio in excess of 1. Unstable isotopes, or **radioisotopes** as they are more commonly known, are often produced artificially, but many occur in nature. Radioisotopes emit particles and/or electromagnetic radiation as a result of changes in the composition of the atomic nucleus. These processes, which are known as **radioactive decay**, arise, either directly or as a result of a decay series, in the production of a stable isotope.

### 14.1.3 Types of radioactive decay

There are several types of radioactive decay; only those most relevant to biochemists are considered below. A summary of properties is given in Table 14.1.

#### Decay by negatron emission

In this case a neutron is converted to a proton by the ejection of a negatively charged **beta ( $\beta$ ) particle** called a **negatron ( $\beta^-$ )**:



To all intents and purposes a negatron is an electron, but the term negatron is preferred, although not always used, since it serves to emphasise the nuclear origin of the particle. As a result of negatron emission, the nucleus loses a neutron but gains a proton. The  $N/Z$  ratio therefore decreases while  $Z$  increases by 1 and  $A$  remains constant. An isotope frequently used in biological work that decays by negatron emission is  $^{14}\text{C}$ .



Negatron emission is very important to biochemists because many of the commonly used radionuclides decay by this mechanism. Examples are:  $^3\text{H}$  and  $^{14}\text{C}$ , which can be used to label any organic compound;  $^{35}\text{S}$  used to label methionine, for example to study protein synthesis; and  $^{32}\text{P}$ , a powerful tool in molecular biology when used as a nucleic acid label.

#### Decay by positron emission

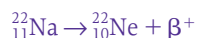
Some isotopes decay by emitting positively charged  $\beta$ -particles referred to as **positrons ( $\beta^+$ )**. This occurs when a proton is converted to a neutron:



### 14.1 The nature of radioactivity

Positrons are extremely unstable and have only a transient existence. Once they have dissipated their energy they interact with electrons and are annihilated. The mass and energy of the two particles are converted to two  $\gamma$ -rays emitted at  $180^\circ$  to each other. This phenomenon is frequently described as **back-to-back emission**.

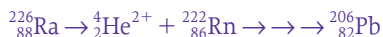
As a result of positron emission the nucleus loses a proton and gains a neutron, the  $N/Z$  ratio increases,  $Z$  decreases by 1 and  $A$  remains constant. An example of an isotope decaying by positron emission is  $^{22}\text{Na}$ :



Positron emitters are detected by the same instruments used to detect  $\gamma$ -radiation. They are used in biological sciences to spectacular effect in brain scanning with the technique **positron emission tomography** (PET scanning) used to identify active and inactive areas of the brain.

#### Decay by alpha particle emission

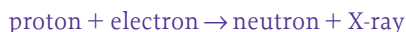
Isotopes of elements with high atomic numbers frequently decay by emitting **alpha ( $\alpha$ ) particles**. An  $\alpha$ -particle is a helium nucleus; it consists of two protons and two neutrons ( $^4\text{He}^{2+}$ ). Emission of  $\alpha$ -particles results in a considerable lightening of the nucleus, a decrease in atomic number of 2 and a decrease in the mass number of 4. Isotopes that decay by  $\alpha$ -emission are not frequently encountered in biological work. Radium-226 ( $^{226}\text{Ra}$ ) decays by  $\alpha$ -emission to radon-222 ( $^{222}\text{Rn}$ ), which is itself radioactive. Thus begins a complex **decay series**, which culminates in the formation of  $^{206}\text{Pb}$ :



Alpha emitters are extremely toxic if ingested, due to the large mass and the ionising power of the atomic particle.

#### Electron capture

In this form of decay a proton captures an electron orbiting in the innermost K shell:



The proton becomes a neutron and electromagnetic radiation (**X-rays**) is given out. Example:



#### Decay by emission of $\gamma$ -rays

In contrast to emission of  $\alpha$ - and  $\beta$ -particles,  **$\gamma$ -emission** involves electromagnetic radiation similar to, but with a shorter wavelength than, X-rays. These  **$\gamma$ -rays** result from a transformation in the nucleus of an atom (in contrast to X-rays, which are emitted as a consequence of excitation involving the orbital electrons of an atom) and frequently accompany  $\alpha$ - and  $\beta$ -particle emission. Emission of  $\gamma$ -radiation in itself leads to no change in atomic number or mass.

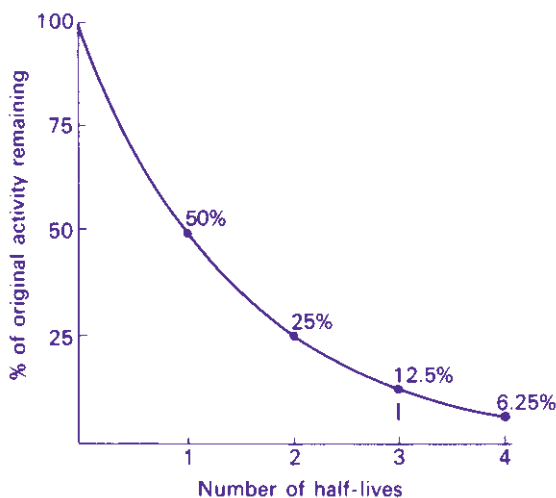


Fig. 14.1. Demonstration of the exponential nature of radioactive decay.

$\gamma$ -Radiation has low ionising power but high penetration. For example, the  $\gamma$ -radiation from  $^{60}\text{Co}$  will penetrate 15 cm of steel. The toxicity of  $\gamma$ -radiation is similar to that of X-rays.

Example:



#### 14.1.4 Radioactive decay energy

The usual unit used in expressing energy levels associated with radioactive decay is the **electron volt**. (One electron volt (eV) is the energy acquired by one electron in accelerating through a potential difference of 1 V and is equivalent to  $1.6 \times 10^{-19}$  J.) For the majority of isotopes, the term **million or mega electron volts** (MeV) is more applicable. Isotopes emitting  $\alpha$ -particles are normally the most energetic, falling in the range 4.0–8.0 MeV, whereas  $\beta$ - and  $\gamma$ -emitters generally have decay energies of less than 3.0 MeV.

#### 14.1.5 Rate of radioactive decay

Radioactive decay is a spontaneous process and it occurs at a definite rate characteristic of the source. This rate always follows an exponential law. Thus the number of atoms disintegrating at any time is proportional to the number of atoms of the isotope ( $N$ ) present at that time ( $t$ ). Expressed mathematically, the exponential curve (Fig. 14.1) gives the equation.

$$-\frac{dN}{dt} \propto N$$



**Table 14.2** Half-lives of some isotopes used in biological studies

Isotope	Half-life
$^3\text{H}$	12.26 years
$^{14}\text{C}$	5760 years
$^{22}\text{Na}$	2.58 years
$^{32}\text{P}$	14.20 days
$^{33}\text{P}$	25.4 days
$^{35}\text{S}$	87.20 days
$^{42}\text{K}$	12.40 h
$^{45}\text{Ca}$	165 days
$^{59}\text{Fe}$	45 days
$^{125}\text{I}$	60 days
$^{131}\text{I}$	8.05 days
$^{135}\text{I}$	9.7 h

$$\text{or } -\frac{dN}{dt} = \lambda N \quad (14.1)$$

where  $\lambda$  is the **decay constant**, a characteristic of a given isotope defined as the fraction of an isotope decaying in unit time ( $t^{-1}$ ). By integrating equation 14.1 it can be converted to a logarithmic form:

$$\ln \frac{N_t}{N_0} = -\lambda t \quad (14.2)$$

where  $N_t$  is the number of radioactive atoms present at time  $t$ , and  $N_0$  is the number of radioactive atoms originally present. In practice it is more convenient to express the decay constant in terms of **half-life** ( $t_{1/2}$ ). This is defined as the time taken for the activity to fall from any value to half that value (Fig. 14.1). If  $N_t$  in equation 14.2 is equal to one-half of  $N_0$  then  $t$  will equal the half-life of the isotope. Thus

$$\ln \frac{1}{2} = -\lambda t_{1/2} \quad (14.3)$$

$$\text{or } 2.303 \log (1/2) = -\lambda t_{1/2} \quad (14.4)$$

$$\text{or } t_{1/2} = 0.693/\lambda \quad (14.5)$$

The values of  $t_{1/2}$  vary widely from over  $10^{19}$  years for lead-204 ( $^{204}\text{Pb}$ ) to  $3 \times 10^{-7}$  s for polonium-212 ( $^{212}\text{Po}$ ). The half-lives of some isotopes frequently used in biological work are given in Table 14.2. Note that two important elements, oxygen and nitrogen, are missing from the table. This is because the half-lives of radioactive isotopes of these elements are too short for most biological studies ( $^{15}\text{O}$  has a  $t_{1/2}$  of 2.03 min, whereas  $^{13}\text{N}$  has a  $t_{1/2}$  of 10.00 min). The advantages and disadvantages of working with isotopes of differing half-lives are given in Table 14.3.

**Table 14.3** The advantages and disadvantages of working with a short half-life isotope

Advantages	Disadvantages
High specific activity (see Section 14.3.4) makes the experiment more sensitive	Experimental design, isotope decays during time of experiment
Easier and cheaper to dispose of	Cost of replacement for further experiments
Lower doses likely (e.g. in diagnostic testing of human subjects)	Frequently need to calculate amount of activity remaining

**Example 1 THE EFFECT OF HALF-LIFE****Question**

Given  $\ln(N_t/N_0) = -\lambda t$  and that the half-life of  $^{32}\text{P}$  is 14.2 days, how long would it take a solution containing 42 000 d.p.m. of  $^{32}\text{P}$  to decay to 500 d.p.m.?

**Answer**

Use equation 14.5 to calculate the value of  $\lambda$ . This gives a value of  $0.0488 \text{ days}^{-1}$ . Then use equation 14.2 to calculate the time taken for the counts to decrease. In this equation  $N_0 = 42\,000$  and  $N_t = 500$ . This gives a value for  $t$  of 90.8 days.

**14.1.6 Units of radioactivity**

The Syst eme International d'Unit es (SI system) uses the **becquerel** (Bq) as the unit of radioactivity. This is defined as one **disintegration per second** (1 d.p.s.). However, an older unit, not in the SI system and still frequently used is the **curie** (Ci). This is defined as the quantity of radioactive material in which the number of nuclear disintegrations per second is the same as that in 1 g of radium, namely  $3.7 \times 10^{10}$  (or 37 GBq, see Table 14.10). For biological purposes this unit is too large and the microcurie ( $\mu\text{Ci}$ ) and millicurie (mCi) are used. It is important to realise that the curie refers to the number of disintegrations actually occurring in a sample (i.e. d.p.s.) not to the disintegrations detected by the radiation counter, which will generally be only a proportion of the disintegrations occurring and are referred to as **counts** (i.e. c.p.s.).

Normally, in experiments with radioisotopes, a carrier of the stable isotope of the element is added. It therefore becomes necessary to express the amount of radioisotope present per unit mass. This is the **specific activity**. It may be expressed in a number of ways including disintegration rate (d.p.s. or d.p.m.), count rate (c.p.s. or c.p.m.) or curies (mCi or  $\mu\text{Ci}$ ) per unit of mass of mixture (units of mass are normally either moles or grams). An alternative method of expressing specific activity, which is not very frequently used, is **atom percentage excess**. This is defined as the number of radioactive atoms per total of 100 atoms of the compound. For quick reference, a list of units and definitions frequently used in radiobiology is provided in Table 14.10.

**14.1.7 Interaction of radioactivity with matter** **$\alpha$ -Particles**

These particles have a very considerable energy (3–8 MeV) and all the particles from a given isotope have the same amount of energy. They react with matter in

two ways. First, they may cause **excitation**. In this process energy is transferred from the  $\alpha$ -particle to orbital electrons of neighbouring atoms, these electrons being elevated to higher orbitals. The  $\alpha$ -particle continues on its path with its energy reduced by a little more than the amount transferred to the orbital electron. The excited electron eventually falls back to its original orbital, emitting energy as **photons** of light in the visible or near visible range. Secondly,  $\alpha$ -particles may cause **ionisation** of atoms in their path. When this occurs the target orbital electron is removed completely. Thus the atom becomes ionised and forms an ion-pair, consisting of a positively charged ion and an electron. Because of their size, slow movement and double positive charge,  $\alpha$ -particles frequently collide with atoms in their path. Therefore they cause intense ionisation and excitation and their energy is rapidly dissipated. Thus, despite their initial high energy,  $\alpha$ -particles are not very penetrating.

### Negatrons

Compared with  $\alpha$ -particles, negatrons are very small and rapidly moving particles that carry a single negative charge. They interact with matter to cause ionisation and excitation exactly as with  $\alpha$ -particles. However, due to their speed and size, they are less likely than  $\alpha$ -particles to interact with matter and therefore are less ionising and more penetrating than  $\alpha$ -radiation. Another difference between  $\alpha$ -particles and negatrons is that, whereas for a given  $\alpha$ -emitter all the particles have the same energy, negatrons are emitted over a range of energy, i.e. negatron emitters have a characteristic **energy spectrum** (see Fig. 14.5b). The **maximum energy level** ( $E_{\max}$ ) varies from one isotope to another, ranging from 0.018 MeV for  ${}^3\text{H}$  to 4.81 MeV for  ${}^{38}\text{Cl}$ . The difference in  $E_{\max}$  affects the penetration of the radiation:  $\beta$ -particles from  ${}^3\text{H}$  can travel only a few millimetres in air, whereas those from  ${}^{32}\text{P}$  can penetrate over 1 m of air. The reason for negatrons of a given isotope being emitted within an energy range was explained by W. Pauli in 1931, when he postulated that each radioactive event occurs with an energy equivalent to  $E_{\max}$  but that the energy is shared between a negatron and a neutrino. The proportion of total energy taken by the negatron and the neutrino varies for each disintegration. Neutrinos have no charge and negligible mass and do not interact with matter.

### $\gamma$ -Rays and X-rays

These rays (henceforth collectively referred to as  $\gamma$ -rays for simplicity) are electromagnetic radiation and therefore have no charge or mass. They rarely collide with neighbouring atoms and travel great distances before dissipating all their energy (i.e. they are highly penetrating). They interact with matter in many ways. The three most important ways lead to the production of secondary electrons, which in turn cause excitation and ionisation. In photoelectric absorption, low energy  $\gamma$ -rays interact with orbital electrons, transferring all their energy to the electron, which is then ejected as a **photoelectron**. The photoelectron subsequently behaves as a negatron. In contrast, **Compton scattering**, which is caused by medium energy  $\gamma$ -rays, results in only part of the energy being transferred to the target electron, which is ejected. The  $\gamma$ -ray is deflected and moves on with reduced energy. Again

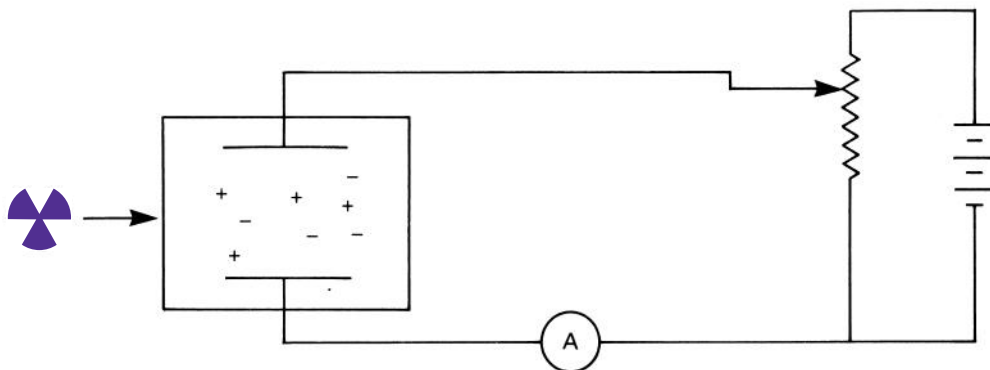


Fig. 14.2. Detection based on ionisation.

the ejected electron behaves as a negatron. **Pair production** results when very high energy  $\gamma$ -rays react with the nucleus of an atom and all the energy of the  $\gamma$ -ray is converted to a positron and a negatron.

When high atomic number materials absorb high energy  $\beta$ -particles, the absorber gives out a secondary radiation, an X-ray called **Bremsstrahlung**. For this reason, shields for  $^{32}\text{P}$  use low atomic number materials such as Perspex.

## 14.2 DETECTION AND MEASUREMENT OF RADIOACTIVITY

There are three commonly used methods of detecting and quantifying radioactivity. These are based on the ionisation of gases, on the excitation of solids or solutions, and the ability of radioactivity to expose photographic emulsions, i.e. autoradiography.

### 14.2.1 Methods based upon gas ionisation

#### The effect of voltage upon ionisation

As a charged particle passes through a gas, its electrostatic field dislodges orbital electrons from atoms sufficiently close to its path and causes ionisation (Fig. 14.2). The ability to induce ionisation decreases in the order

$$\alpha > \beta > \gamma \quad (10\,000 : 100 : 1)$$

Accordingly,  $\alpha$ - and  $\beta$ -particles may be detected by gas ionisation methods, but these methods are poor for detecting  $\gamma$ -radiation. If ionisation occurs between a pair of electrodes enclosed in a suitable chamber, a pulse (current) flows, the magnitude of which is related to the applied potential and the number of radiation particles entering the chamber (Fig. 14.3). The various 'regions' shown in Fig. 14.3 will now be considered.

In the **ionisation chamber region** of the curve, each radioactive particle produces only one ion-pair per collision. Hence the currents are low, and very

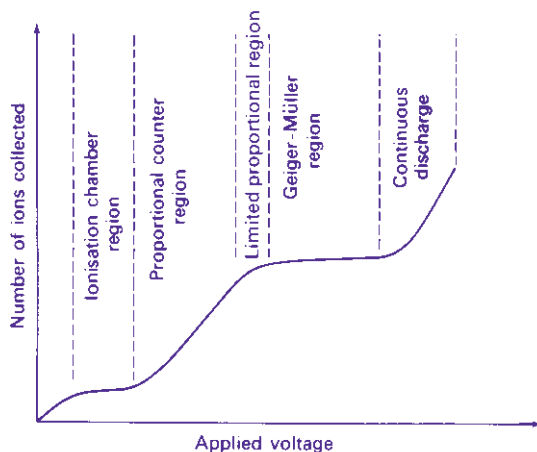


Fig. 14.3. Effect of voltage on pulse flow.

sensitive measuring devices are necessary. This method is little used in quantitative work, but various types of electroscopes, which operate on this principle, are useful in demonstrating the properties of radioactivity. At a higher voltage level than that of the simple ionisation chambers, electrons resulting from ionisation move towards the anode much more rapidly; consequently they cause secondary ionisation of gas in the chamber, resulting in the production of secondary ionisation electrons, which cause further ionisation and so on. Hence from the original event a whole torrent of electrons reaches the anode. This is the principle of gas amplification and is known as the **Townsend avalanche effect**, after its discoverer. As a consequence of this gas amplification, current flow is much greater. As can be seen in Fig. 14.3, in the **proportional counter region** the number of ion-pairs collected is directly proportional to the applied voltage until a certain voltage is reached, when a plateau occurs. Before the plateau is reached there is a region known as the **limited proportional region**, which is not often used in detection and quantification of radioactivity and hence will not be discussed.

The main drawback of counters that are manufactured to operate in the **proportional region** is that they require a very stable voltage supply because small fluctuations in voltage result in significant changes in amplification. Proportional counters are particularly useful for detection and quantification of  $\alpha$ -emitting isotopes, but it should be noted that relatively few such isotopes are used in biological work.

In the **Geiger-Müller region** all radiation particles, including weak  $\beta$ -particles, induce complete ionisation of the gas in the chamber. Thus the size of the current is no longer dependent on the number of primary ions produced. Since maximal gas amplification is realised in this region, the size of the output pulse from the detector will remain the same over a considerable voltage range (the so-called **Geiger-Müller plateau**). The number of times this pulse is produced is measured rather than its size. Therefore it is not possible to discriminate between different isotopes using this type of counter.

Since it takes a finite time for the ion-pairs to travel to their respective electrodes, other ionising particles entering the tube during this time fail to produce ionisation and hence are not detected, thereby reducing the counting efficiency. This is referred to as the **dead time** of the tube and is normally 100 to 200  $\mu\text{s}$ . When the ions reach the electrode they are neutralised. Inevitably some escape and produce their own ionisation avalanche. Thus, if unchecked, a Geiger–Müller tube would tend to give a continuous discharge. To overcome this, the tube is quenched by the addition of a suitable gas, which reduces the energy of the ions. Common quenching agents are ethanol, ethyl formate and the halogens.

### Example 2 THE EFFECT OF DEAD TIME

#### Question

What do you think will happen to the counting efficiency of a Geiger–Müller counter as the count rate rises?

#### Answer

The efficiency will fall since there will be an increased likelihood that two or more  $\beta$ -particles will enter the tube during the dead time.

#### Instrumentation

Counters based on gas ionisation used to be the main method employed in the quantification of radioisotopes in biological samples. Currently, **scintillation counting** (Section 14.2.2) has virtually taken over. However, all laboratories use small hand-held radioactivity monitors based on gas ionisation, the end-window design being the most popular type (Fig. 14.4). These counters have a thin end-window made from aluminium and can detect  $\beta$ -radiation from high energy ( $^{32}\text{P}$ ) and weak emitters ( $^{14}\text{C}$ ), but are incapable of detecting  $^3\text{H}$  because the radiation cannot penetrate the end-window. For the same reason they are not very efficient detectors of  $\alpha$ -radiation.

End-window ionisation counters are used for routine monitoring of the radioactive laboratory to check for contamination. They are also useful in experimental situations where the presence or absence of radioactivity needs to be known rather than the absolute quantity, for example quick screening of radioactive gels prior to autoradiography or checking of chromatographic fractions for labelled components.

The inability of end-window counters to detect weak  $\beta$ -emitters presents a problem in biosciences because  $^3\text{H}$  is a very commonly used radioisotope. The problem can be overcome by using a so-called windowless counter where a gas flow is used. These instruments are rather cumbersome and need to be carried around on an object that resembles a golf trolley. They are useful for mass screening of premises for  $^3\text{H}$  contamination but are rarely used as routine. Most laboratories monitor for  $^3\text{H}$  by doing a **wipe test** regularly, i.e. using wet tissues or cotton wool to take swabs for scintillation counting.

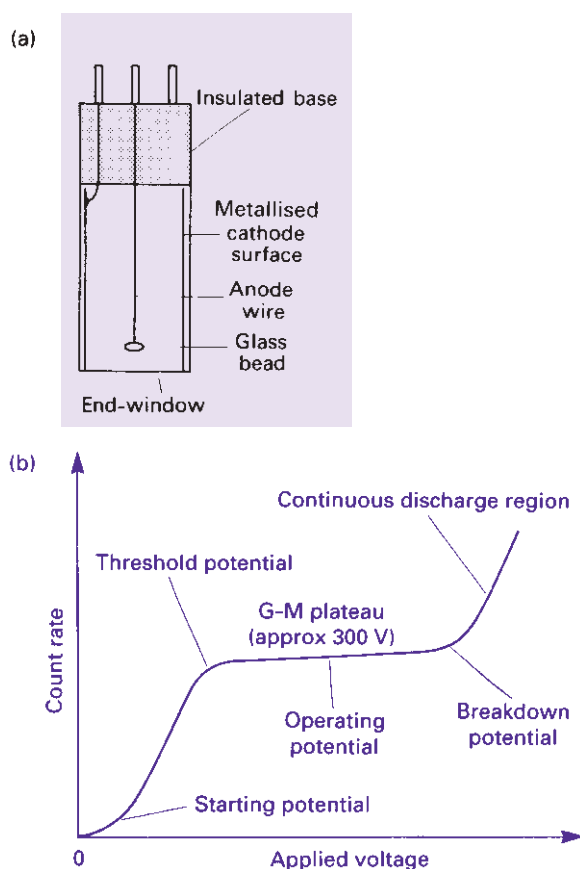


Fig. 14.4. (a) The Geiger-Müller (G-M) tube and (b) the effect of applied voltage on count rate.

### 14.2.2 Methods based upon excitation

As outlined in Section 14.1.7, radioactive isotopes interact with matter in two ways, causing ionisation, which forms the basis of Geiger-Müller counting, and excitation. The latter effect leads the excited compound (known as the fluor) to emit photons of light. This fluorescence can be detected and quantified. The process is known as **scintillation** and when the light is detected by a photomultiplier, forms the basis of scintillation counting. The electric pulse that results from the conversion of light energy to electrical energy in the photomultiplier is directly proportional to the energy of the original radioactive event. This is a considerable asset of scintillation counting, since it means that two, or even more, isotopes can be separately detected and measured in the same sample, provided they have sufficiently different emission energy spectra (see below). The mode of action of a photomultiplier is shown in Fig. 14.5.

In summary, scintillation counting provides information of two kinds:

- *Quantitative:* The number of scintillations is proportional to the rate of decay of the sample, i.e. the amount of radioactivity.

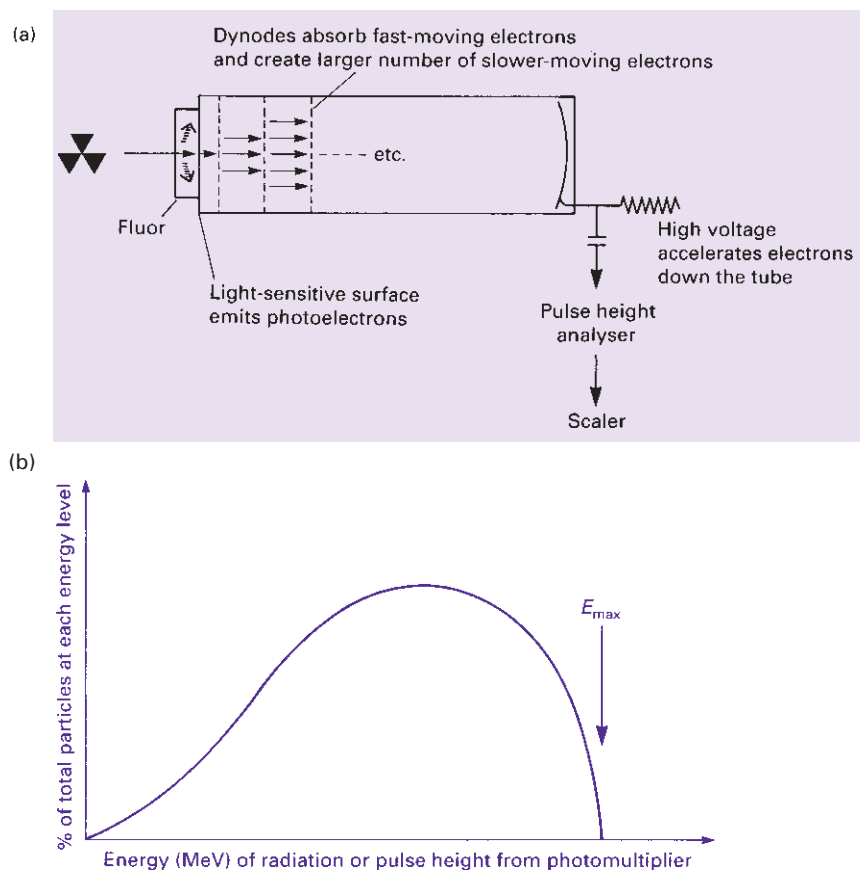


Fig. 14.5. (a) The mode of action of a photomultiplier and (b) the energy spectrum of a typical  $\beta$ -emitter.

- *Qualitative:* The intensity of light given out and therefore signal from the photomultiplier is proportional to the energy of radiation.

### Types of scintillation counting

There are two types of scintillation counting, which are illustrated diagrammatically in Fig. 14.6. In **solid scintillation counting** the sample is placed adjacent to a crystal of fluorescent material. The crystal that is normally used for  $\gamma$ -isotopes is sodium iodide, whereas for  $\alpha$ -emitters zinc sulphide crystals are preferred and for  $\beta$ -emitters organic scintillators such as anthracene are used. The crystals themselves are placed near to a photomultiplier, which in turn is connected to a high voltage supply and a scaler (Fig. 14.6a). Solid scintillation counting is particularly useful for  $\gamma$ -emitting isotopes. This is because, as explained in Section 14.1.7, these rays are electromagnetic radiation and collide only rarely with neighbouring atoms to cause ionisation or excitation. Clearly, in a crystal the atoms are densely packed, making collisions more likely. Conversely, solid scintillation counting is generally unsuitable for weak  $\beta$ -emitting isotopes such as  $^3\text{H}$  and  $^{14}\text{C}$ , because



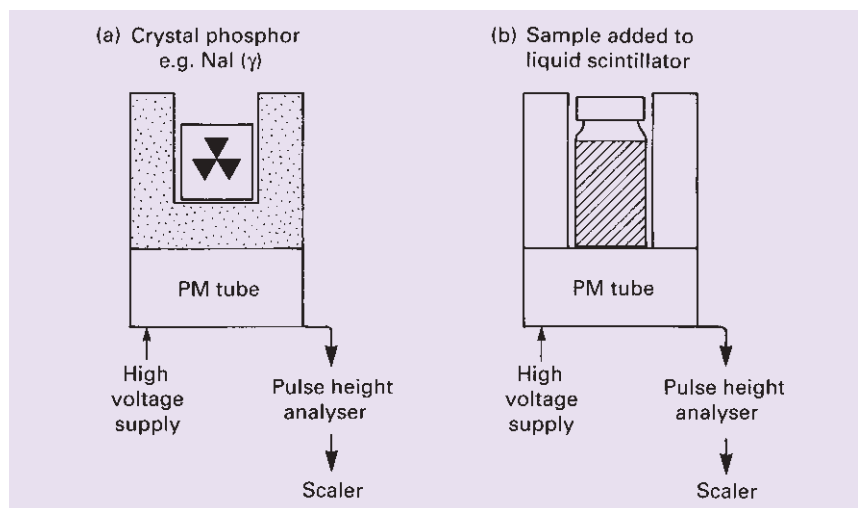


Fig. 14.6. Diagrammatic illustration of solid (a) and liquid (b) scintillation counting methods.

even the highest energy neutrons emitted by these isotopes would have hardly sufficient energy to penetrate the walls of the counting vials in which the samples are placed for counting. As many of the isotopes used in [radioimmunoassay](#) (Section 7.7) are  $\gamma$ -emitting isotopes, solid scintillation counting is frequently used in biological work.

In [liquid scintillation counting](#) (Fig. 14.6b), the sample is mixed with a [scintillation cocktail](#) containing a solvent and one or more fluors. This method is particularly useful in quantifying weak  $\beta$ -emitters such as  $^3\text{H}$ ,  $^{14}\text{C}$  and  $^{35}\text{S}$ , which are frequently used in biological work. For these isotopes, liquid scintillation counting is the usual method. Thus the remainder of this section will place particular emphasis on this technique, though it should be pointed out that most of what follows applies equally to solid scintillation counting used in the quantification of  $\gamma$ -emitters.

### Energy transfer in liquid scintillation counting

A small number of organic solvents fluoresce when bombarded with radioactivity. The light emitted is of very short wavelength (Fig. 14.7) and is not efficiently detected by most photomultipliers. However, if a compound is dissolved that can accept the energy from the solvent and itself fluoresce at a longer wavelength, then the light can be more efficiently detected. Such a compound is known as a [primary fluor](#) and the most frequently used example is 2,5-diphenyl-oxazole (PPO). Unfortunately the light emitted by PPO is not always detected with very high efficiency (depending on the photomultiplier detector) but this can be overcome by including a [secondary fluor](#) or wavelength shifter such as 1,4-bis(5-phenyloxazol-2-yl)benzene (POPOP). Thus the energy transfer process becomes

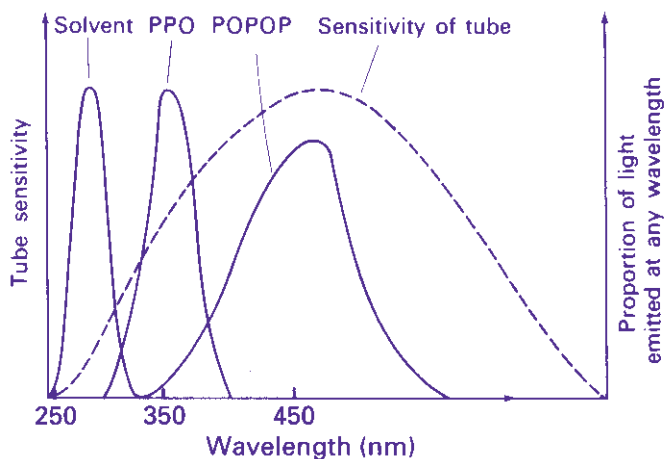
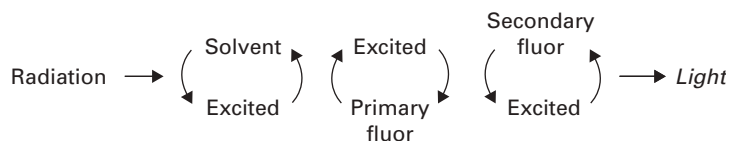


Fig. 14.7. Emission spectra of various fluors in relation to sensitivity of phototubes.



The question obviously arises as to why a primary fluor *and* a secondary fluor are necessary when it is the latter that emits light at the best wavelength for detection. The answer is simply that the solvent cannot transfer its energy directly to the secondary fluor.

PPO and POPOP were among the original fluors used in liquid scintillation counting and remain a favourite choice. However, compounds such as 2-(4'-*t*-butylphenyl)-5-(4''-biphenyl)-1,3,4-oxadiazole (BUTYL-PBD) is a better primary fluor but is quite expensive and is affected by extremes of pH.

Most laboratories now buy their scintillation cocktails already prepared and there are many different makes and recipes on the market. Competition and an increasing awareness of health and safety mean that scintillation cocktails are gradually becoming less toxic and have a lower fire hazard. A final point: some cocktails (as just described) are designed for organic samples and others for aqueous samples (these cocktails include an emulsifier such as the detergent Triton X-100); it is important that the appropriate formulation is used.

#### Advantages of scintillation counting

The very fact that scintillation counting is widely used in biological work indicates that it has several advantages over gas ionisation counting. These advantages are listed below.

- The rapidity of fluorescence decay ( $10^{-9}$  s), which, when compared to dead time in a Geiger–Müller tube ( $10^{-4}$  s), means much higher count rates are possible.
- Much higher counting efficiencies particularly for low energy  $\beta$ -emitters; over 50% efficiency is routine in scintillation counting and efficiency can rise to over 90% for high energy emitters. This is partly due to the fact that the negatrons do not have to travel through air or pass through an end-window of a Geiger–Müller tube (thereby dissipating much of the energy before causing ionisation) but interact directly with the fluor; energy loss before the event that is counted is therefore minimal.
- The ability to accommodate samples of any type, including liquids, solids, suspensions and gels.
- The general ease of sample preparation (see below).
- The ability to count separately different isotopes in the same sample, which means [dual labelling experiments](#) can be carried out (see below).
- Scintillation counters are highly automated, hundreds of samples can be counted automatically and built-in computer facilities carry out many forms of data analysis, such as efficiency correction, graph plotting, radioimmunoassay calculations, etc.

#### Disadvantages of scintillation counting

It would not be reasonable, having outlined some of the advantages of scintillation counting, to disregard the disadvantages of the method. Fortunately, however, most of the inherent disadvantages have been overcome by improvement in instrument design. These disadvantages include the following.

- The cost per sample of scintillation counting is not insignificant; however, other factors including versatility, sensitivity, ease and accuracy outweigh this factor for most applications.
- At the high voltages applied to the photomultiplier, electronic events occur in the system that are independent of radioactivity but contribute to a high background count. This is referred to as photomultiplier noise and can be partially reduced by cooling the photomultipliers. Since temperature affects counting efficiency, cooling also presents a controlled temperature for counting, which may be useful. Low noise photomultipliers, however, have been designed to provide greater temperature stability in ambient temperature systems. Also the use of a [pulse height analyser](#) can be set so as to reject, electronically, most of the noise pulses that are of low energy (the [threshold](#) or [gate setting](#)). The disadvantage here is that this also rejects the low energy pulses resulting from low energy radioactivity (e.g.  $^3\text{H}$ ). Another method of reducing noise, which is incorporated into most scintillation counters, is to use [coincidence counting](#). In this system two photomultipliers are used. These are set in coincidence such that only when a pulse is generated in both tubes at the same time is it allowed to pass to the scaler. The chances of this happening for a pulse generated by a radioactive event is very high compared to the chances of a noise event occurring in both

- photomultipliers during the so-called **resolution time** of the system, which is commonly of the order of 20 ns. In general, this system reduces photomultiplier noise to a very low level.
- The greatest disadvantage of scintillation counting is **quenching**. This occurs when the energy transfer process described earlier suffers interference. Correcting for this quenching contributes significantly to the cost of scintillation counting. Quenching can be any one of three kinds.
    - (i) *Optical quenching*: This occurs if inappropriate or dirty scintillation vials are used. These will absorb some of the light being emitted, before it reaches the photomultiplier.
    - (ii) *Colour quenching*: This occurs if the sample is coloured and results in light emitted being absorbed within the scintillation cocktail before it leaves the sample vial. When colour quenching is known to be a major problem, it can be reduced, as outlined later.
    - (iii) *Chemical quenching*: This form of quenching, which occurs when anything in the sample interferes with the transfer of energy from the solvent to the primary fluor or from the primary fluor to the secondary fluor, is the most difficult form of quenching to accommodate. In a series of homogeneous samples (e.g.  $^{14}\text{CO}_2$  released during metabolism of [ $^{14}\text{C}$ ]glucose and trapped in alkali, which is then added to the scintillation cocktail for counting), chemical quenching may not vary greatly from sample to sample. In these cases relative counting using sample counts per minute can be compared directly. However, in the majority of biological experiments using radioisotopes, such homogeneity of samples is unlikely and it is not sufficiently accurate to use relative counting (i.e. counts per minute). Instead, an appropriate method of standardisation must be used. This requires the determination of the counting efficiency of each sample and the conversion of counts per minute to absolute counts (i.e. disintegrations per minute), as described later. It should be noted that quenching is not such a great problem in solid (external) scintillation counting.
  - *Chemiluminescence*: This can also cause problems during liquid scintillation counting. It results from chemical reactions between components of the samples to be counted and the scintillation cocktail, and produces light emission unrelated to excitation of the solvent and fluor system by radioactivity. These light emissions are generally low energy events and are rejected by the threshold setting of the photomultiplier in the same way as is photomultiplier noise. Chemiluminescence, when it is a problem, can usually be overcome by storing samples for some time before counting, to permit the chemiluminescence to decay. Many contemporaneous instruments are able to detect chemiluminescence and subtract it or flag it on the printout.
  - *Phospholuminescence*: This results from components of the sample, including the vial itself, absorbing light and re-emitting it. Unlike chemiluminescence,

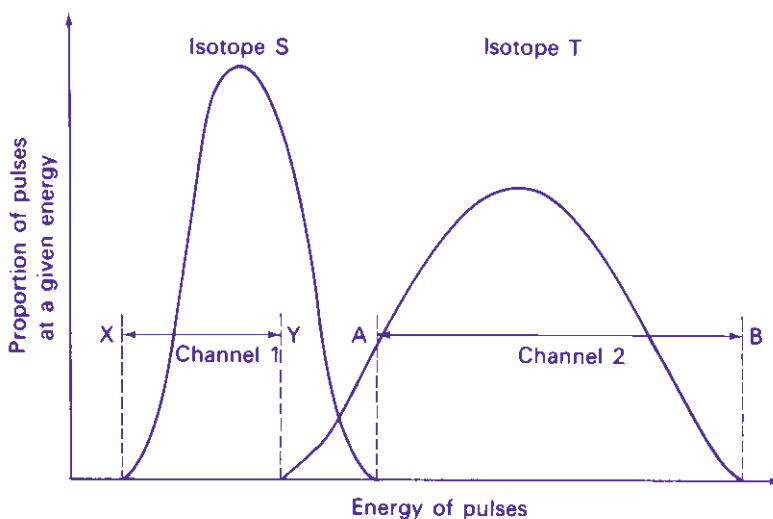


Fig. 14.8. Diagram to illustrate the principle of counting dual-labelled samples.

which is a once-only effect, phospholuminescence will occur on each exposure of a sample to light. Samples that are pigmented are most likely to phosphoresce. If this is a problem, samples should be adapted to dark prior to counting and the sample holder should be kept closed throughout the counting process.

Despite all the complications described above, scintillation counters are universal in biosciences departments. This is because the instruments have automated systems for calculating counting efficiency; in other words, the instruments do all the hard work!

### Using scintillation counting for dual-labelled samples

A feature of the scintillation process is that the size of electric pulse produced by the conversion of light energy in the photomultiplier is related directly to the energy of the original radioactive event. Because different  $\beta$ -emitting isotopes have different energy spectra, it is possible to quantify two isotopes separately in a single sample, provided their energy spectra are sufficiently different. Examples of pairs of isotopes that have sufficiently different energy spectra are  $^3\text{H}$  and  $^{14}\text{C}$ ,  $^3\text{H}$  and  $^{35}\text{S}$ ,  $^3\text{H}$  and  $^{32}\text{P}$ ,  $^{14}\text{C}$  and  $^{32}\text{P}$ ,  $^{35}\text{S}$  and  $^{32}\text{P}$ . The principle of the method is illustrated in Fig. 14.8, where it can be seen that the spectra of two isotopes (S and T) overlap only slightly. By setting a pulse height analyser to reject all pulses of an energy below X (threshold X) and to reject all pulses of an energy above Y (window Y) and also to reject below a threshold of A and a window of B, it is possible to separate the two isotopes completely. A pulse height analyser set with a threshold and window for a particular isotope is known as a **channel** (e.g. a  $^3\text{H}$  channel).

Most modern counters operate with a so-called multichannel analyser. These are based on an analogue-to-digital converter; electronic signals from the

photomultiplier are converted to digital signals stored in a computer. Thus the entire energy spectrum is analysed simultaneously. This greatly facilitates multi-isotope counting and in particular allows the effect of quenching on dual-label counting to be assessed adequately.

Dual-label counting has proved to be useful in many aspects of molecular biology (e.g. nucleic acid hybridisation and transcription), metabolism (e.g. steroid synthesis) and drug development.

#### Determination of counting efficiency

As outlined above, a major problem encountered in scintillation counting is that of quenching, which makes it necessary to determine the **counting efficiency** of some, if not all, of the samples in a particular experiment. This can be done by one of several methods of standardisation, all of which apply to both solid and liquid scintillation counting, though again in this section emphasis is placed on the latter method.

*Internal standardisation* The sample is counted (and gives a reading of, say,  $A$  c.p.m.), removed from the counter and a small amount of standard material of known disintegrations per minute ( $B$  d.p.m.) is added. The sample is then recounted ( $C$  c.p.m.) and the counting efficiency of the sample calculated:

$$\text{counting efficiency} = [100(C - A)/B] \% \quad (14.6)$$

It is obviously necessary in this method to use an **internal standard** (the spike) that contains the same isotope as the one being counted and also to ensure that the standard itself does not act as a quenching agent. Suitable  $^{14}\text{C}$ -labelled standards include  $[^{14}\text{C}]$ toluene,  $[^{14}\text{C}]$ hexadecane,  $[^3\text{H}]$ benzoic acid and  $^3\text{H}_2\text{O}$  (benzoic acid and water are themselves quenching agents and must be used in only very small amounts). Internal standardisation is simple and reliable and corrects adequately for all types of quenching. Carefully carried out, it is the most accurate way of correcting for quenching. On the other hand, it demands very accu-

### Example 3 THE INTERNAL STANDARD METHOD FOR CALCULATING COUNTING EFFICIENCY

#### Question

An experimental sample of  $^3\text{H}$  on a filter paper in scintillation fluid gave a count rate of 1450 c.p.m. in a liquid scintillation counter. The filter was removed and 5064 d.p.m. added to it. On recounting, the filter gave a reading of 2878 c.p.m. What was the d.p.m. of the experimental sample?

#### Answer

It is first necessary to use equation 14.6 to calculate the counting efficiency:

$$\text{counting efficiency} = [100(2878 - 1450)/5064]\%$$

This gives a value of 28.2%. This value is then used to correct the original count figure, i.e.:

$$(1450/28.2)100 = 5142 \text{ d.p.m.}$$

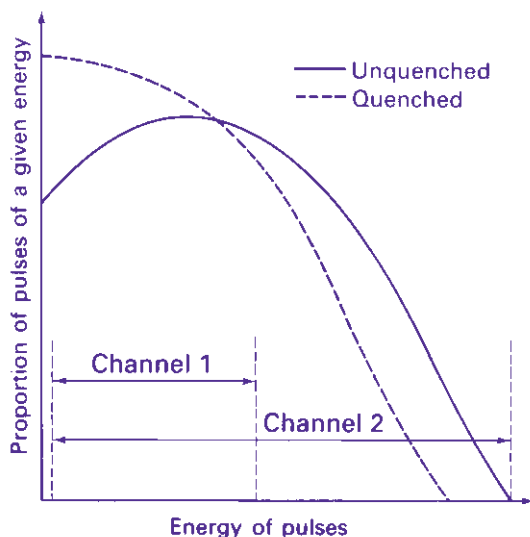


Fig. 14.9. The effect of quenching of a  $\beta$ -energy spectrum.

rate pipetting when the standard is added, and it is time consuming because each sample must be counted twice. It also means that the sample cannot be recounted in the event of error because it will be contaminated with the standard. Moreover, time elapses between the first and second count and changes in sample quenching characteristics can also occur, which can lead to considerable inaccuracies. However, it is the means by which the following two methods are calibrated.

**Channels ratio** When a sample in a scintillation counter is quenched, the scintillation process is less efficient: less light is produced for a given quantum energy of radiation. Thus the energy spectrum for a quenched sample appears to be lower than for an unquenched sample (Fig. 14.9). The higher the degree of quenching, the more pronounced is the resulting decrease in the spectrum. This fact is made use of in the channels ratio method for determining counter efficiency. The method involves the preparation of a calibration curve based on counting in two channels that cover different, but overlapping, parts of the spectrum. As a sample is quenched, and the spectrum shifts to gradually lower apparent energies, the ratio of counts in each channel will vary. To prepare the standard curve, a set of quenched standards is counted: the absolute amount of radioactivity is known and therefore the efficiency of counting in each channel can easily be determined.

The efficiency is then plotted against channels ratio to form the standard curve (Fig. 14.10). Typical data for a set of  $^{14}\text{C}$  quenched standards are given in Table 14.4. It is important to realise that a standard curve applies to only one set of circumstances – one radioisotope, counter and scintillation fluid.

Once the standard curve has been prepared, the efficiency of counting experimental samples can be determined. Samples are counted in the same two channels, the ratio is calculated, put into the graph and the efficiency read. In practice all

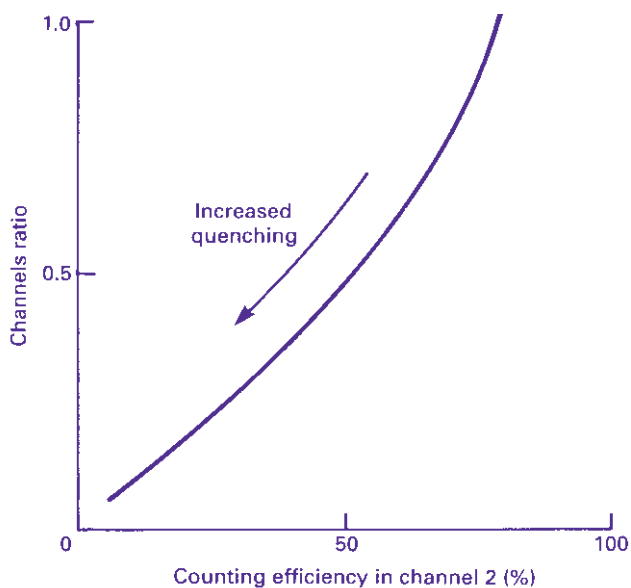


Fig. 14.10. Channels ratio quench correction curve.

**Table 14.4** Radioactivity recorded with gradually increasing quench in two channels of a scintillation counter

Sample	c.p.m.		Ratio	Counting efficiency in channel 2 (%)
	Channel 1	Channel 2	Ch1 : Ch2	
<sup>14</sup> C standard (203 600 d.p.m.) unquenched	171 930	184 250	0.93	90.5
<sup>14</sup> C standard (203 600 d.p.m.) with increasing quench	146 610	168 840	0.87	82.9
	94 240	135 090	0.70	66.3
	52 260	102 030	0.51	50.1
	16 030	58 320	0.27	28.6
	5 920	34 740	0.17	17.1
	2 060	20 270	0.10	9.9
	1 130	13 260	0.08	6.5

the data can be stored in the counter's computer and corrected values printed automatically.

Multichannel scintillation counters operate on the same principle but the whole shape and position of the spectrum is analysed. This is given a digital parameter that relates to counting efficiency. Manufacturers have developed their own titles for such parameters, for example LKB Instruments' *Automatic Quench Compensation* or Packard's *Automatic Efficiency Control*. These systems have greater precision than the two-channel approach, as the whole of the spectrum is used for analysis. The channels ratio method is suitable for all types and even high degrees of quenching. Furthermore, counting in more than one channel is



simultaneous and this method is, therefore, less time consuming than either internal or external standardisation. It is also, in practice, an acceptably accurate method for determining counting efficiency, provided care is taken in the preparation of the calibration curve. However, it is notoriously inaccurate at low count rates, because the error on the counts per minute is high and there will be a larger error on the channels ratio because it is calculated from two values of the counts per minute. It is also inaccurate for very highly quenched samples. For these reasons the method that follows is most frequently the procedure of choice.

#### Example 4 CHANNELS RATIO EFFICIENCY CALCULATION

##### Question

The efficiency of counting 100 000 d.p.m. of a [<sup>14</sup>C]leucine solution was estimated in a scintillation counter using two channels, A and B, in scintillation fluid containing increasing amounts of chloroform. The following data were obtained:

Chloroform (cm <sup>3</sup> )	c.p.m. A	c.p.m. B
0	48 100	54 050
1	31 612	42 150
2	17 608	28 400
3	7 400	15 000

An unknown sample of [<sup>14</sup>C]leucine gave the following data:

Channel A 1890 c.p.m.  
Channel B 2700 c.p.m.

How much radioactivity is present in the unknown sample?

##### Answer

Plot efficiency in channel A or B (e.g.  $48\,000 \times 100/100\,000$  or  $54\,050 \times 100/100\,000$ , then  $31\,612 \times 100/100\,000$  or  $42\,150 \times 100/100\,000$  etc.) against c.p.m. A/c.p.m. B (e.g.  $48\,000/54\,050$ , then  $31\,612/42\,150$ , etc.). Calculate c.p.m. A/c.p.m. B for the experimental sample ( $1890/2700$ ), put this into your graph and read off the efficiency. Correct the c.p.m. in channel A or B (depending on which one you choose to calculate efficiencies) for the efficiency (e.g.  $1980 \times 100/26.5$  if you used channel A (26.5% is the efficiency obtained from the graph of channels ratio against efficiency in channel A)).

Try plotting two graphs (efficiency in A or B versus c.p.m. A/c.p.m. B) and work out the answer using both in turn; you should get the same answer of 7130 d.p.m. each time.

*External standardisation* Instruments have a  $\gamma$ -emitting external standard built into the counter. Under the control of the counter each sample to be counted is exposed to this external source, which is automatically shifted from a lead shield to the counting chamber. The  $\gamma$ -radiation penetrates the vial and excites the scintillation fluid. The resulting spectrum is unique to the source and is significantly different from that produced by the sample in the vial. The  $\gamma$ -source

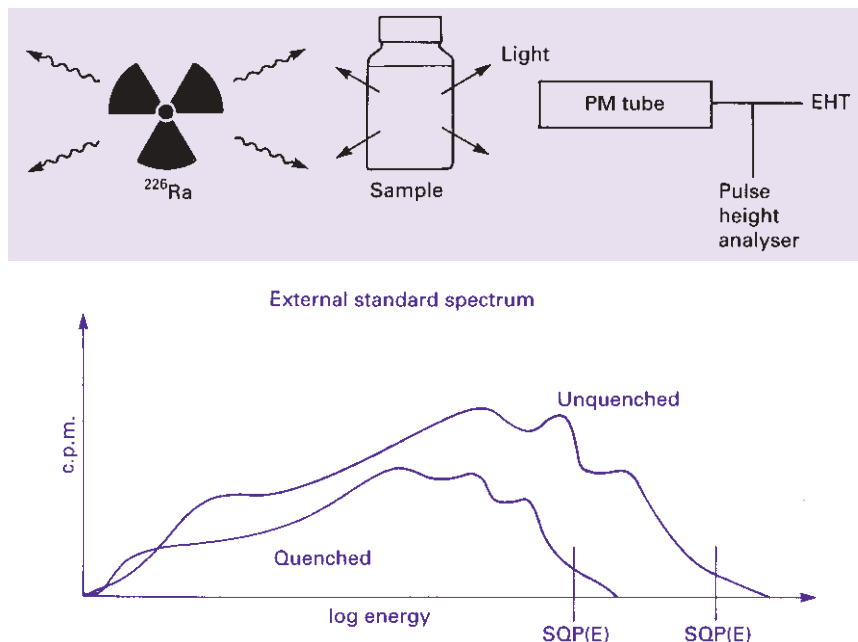


Fig. 14.11. The external standard for estimating counting efficiency. The external source irradiates the sample. The counter analyses the spectrum, which shifts to lower energies if the sample is quenched. The SQP(E), i.e. standard quench parameter (external), expressed without units, is derived from the energy axis and relates to the extent of quench. The greater the quench in the sample, the lower the SQP(E) and the lower the counting efficiency (see Table 14.5).

used (e.g.  $^{137}\text{Cs}$ ,  $^{133}\text{Ba}$  or  $^{226}\text{Ra}$ ) varies according to the make of instrument. The spectrum obtained by  $^{226}\text{Ra}$  is shown in Fig. 14.11.

Quenching agents present in the scintillation fluid will significantly affect the spectrum obtained. The instrument analyses this spectrum and assigns a quench parameter to it. The precise method used depends on the make of counter; LKB Instruments refer to a standard quench parameter for the external source (SQP(E)) based on a point on the energy axis (Fig. 14.11). Other manufacturers use slightly different approaches but the principle is the same: the spectrum for the external standard varies according to the degree of quench in the vial and, therefore, the efficiency of counting of the internal experimental sample.

As for the channels ratio method, a standard curve is required, i.e. a range of quenched standards is counted and the external standard spectrum analysed in each case. The resulting data (Table 14.5) are used to prepare a standard curve that is held in the instrument's computer. Unknown samples are then counted in the same way, the efficiency read from the standard curve and the sample counts corrected.

The external standard approach is now routine in most laboratories, the main advantage over the channels ratio method being that it is suited to samples with low count rates. However, it is not without disadvantages: a standard curve is required for each set of circumstances (as with the channels ratio) and the user can

**Table 14.5** Recorded radioactivity from a  $^{14}\text{C}$  standard sample with increasing quench detected by an external standard

Sample	c.p.m.	External quench parameter <sup>a</sup>	Counting efficiency (%)
$^{14}\text{C}$ standard (203 600 d.p.m.) unquenched	194 930	810	95.7
$^{14}\text{C}$ standard (203 600 d.p.m.) with increasing quench	146 141	422	93.5
	181 171	207	89.0
	167 731	126	82.4
	145 879	76	71.6
	126 913	55	62.3
	108 641	42	53.3
	96 103	37	47.2

<sup>a</sup> e.g. SQP(E), see Fig. 14.11.

be lulled into a false sense of security. The system is so highly automated that it is easy to lose sight of the basic principles and the method is not always appropriate. A case in point is the counting of  $^3\text{H}$  precipitated onto filters counted in scintillation fluid. The external standard method will calculate the degree of quench in the fluid (which will probably be very low) but will not take into account the poor penetration of  $^3\text{H}$   $\beta$ -particles from the filter into the scintillation fluid: artificially high efficiencies will be recorded.

In all cases where an automated procedure for calculating counting efficiencies is employed it is prudent to count a few prepared samples in which the true amount of radioactivity is known.

### Example 5 EXTERNAL STANDARD EFFICIENCY CALCULATIONS

#### Question

The efficiency of detecting  $^{14}\text{C}$  in a scintillation counter was determined by counting a standard sample containing 105 071 d.p.m. at different degrees of quench analysed by the external standard approach:

c.p.m.	SQP
87 451	0.90
62 361	0.64
45 220	0.46
21 014	0.21

SQP, standard quench parameter.

An experimental sample gave 2026 c.p.m. at an SQP of 0.52. What is the true count rate?

#### Answer

Plot the efficiency (e.g.  $(87\,451 \times 100/105\,071)\%$ ) versus SQP. Obtain the efficiency (48%) for the experimental sample and correct 2026 to give an answer of 4221 d.p.m.

### Sample preparation

It is impossible here to give details of all aspects of sample preparation for scintillation counting. However, major considerations are outlined below and the reader is referred to books cited in Section 14.7 for further details.

*Sample vials* In solid scintillation counting, sample preparation is easy and only involves transferring the sample to a glass or plastic vial (or tube) compatible with the counter. In liquid scintillation counting, sample preparation is more complex and starts with a decision on the type of sample vial to be used. These may be glass, low potassium glass (with low levels of  $^{40}\text{K}$  that reduce background count) or polyethylene. The last of these types are cheaper but are not suitable for cleaning and reuse, whereas glass vials can be reused many times provided they are thoroughly cleaned. Polyethylene vials give better light transfer and result in slightly higher counting efficiencies, but are inclined to exhibit more phosphorescence than do glass vials. The recent trend is towards mini-vials, which use far smaller volumes of expensive scintillation cocktails. Modern counters are able to accept many types of vial; the smallest vial possible should be used (within the obvious constraints of sample volume) to save costs and in consideration of environmental issues, as scintillation fluids are toxic. Some counters are designed to accept very small samples in special polythene bags split into an array of many compartments; these are particularly useful to, for example, the pharmaceutical industry where there are laboratories that do large numbers of receptor binding assays.

*Scintillation cocktails* Toluene-based cocktails are the most efficient, but will not accept aqueous samples, because toluene and water are immiscible and massive quenching results. Cocktails based on 1,4-dioxane and naphthalene that can accommodate up to 20% (v/v) water can be used, but they have largely been phased out due to toxicity. Emulsifier-based cocktails are the most frequently used for counting aqueous samples. They contain an emulsifier such as Triton X-100 and can accept up to 50% water (v/v); however, phase transitions occur from single phase to two phase or gel, as the water content increases. Accurate counting cannot be done if the samples are in the two-phase state. Many ready-made cocktails are on the market and are sold with precise instructions regarding sample condition.

*Volume of cocktail* It should be noted that the efficiency of scintillation counting varies with sample volume, though this is less of a problem in modern counters. Nevertheless, care should be taken that sample vials in a given series of counts contain the same volume of sample and that all instrument calibration is done using the same volume as for experimental samples.

*Overcoming major colour quenching* If colour quenching is a problem it is possible to bleach samples before counting. Care should be taken, however, since bleaching agents such as hydrogen peroxide can give rise to chemiluminescence in some scintillation cocktails.

**Table 14.6** Some isotopes suitable for Čerenkov counting

Radioisotope	$E_{\max}$ (MeV)	% of spectrum above 0.5 MeV	Counting efficiency (%)
$^{22}\text{Na}$	1.39	60	30
$^{32}\text{P}$	1.71	80	40
$^{36}\text{Cl}$	0.71	30	10
$^{42}\text{K}$	3.5	90	80

*Tissue solubilisers* Solid samples, such as plant and animal tissues, may be best counted after solubilisation by quaternary amines such as NCS solubiliser or Soluene. Not surprisingly these solutions are highly toxic and great care is required. The sample is added to the counting vial containing a small amount of solubiliser and digestion is allowed to proceed. When digestion is complete, scintillation cocktail is added and the sample counted. Again, chemiluminescence can be a problem with tissue solubilisers.

*Combustion methods* A suitable alternative to bleaching of coloured samples or digestion of tissues is the use of combustion techniques. Here samples are combusted in an atmosphere of oxygen, usually in a commercially available combustion apparatus. Thus samples containing  $^{14}\text{C}$  would be combusted to  $^{14}\text{CO}_2$ , which is collected in a trapping agent such as sodium hydroxide and then counted;  $^3\text{H}$ -containing samples are converted to  $^3\text{H}_2\text{O}$  for counting.

As indicated earlier, only important considerations in sample preparation are discussed above and details are not given. However, it is worthy of comment that almost any type of radioactive sample containing  $\beta$ -emitting isotopes can be prepared for counting in a liquid scintillation counter by one method or another, including cuttings from paper chromatographs or membrane filters, again illustrating the versatility and importance of this technique for quantifying radioactivity.

### Čerenkov counting

The Čerenkov effect occurs when a particle passes through a substance with a speed higher than that of light passing through the same substance. If a  $\beta$ -emitter has a decay energy in excess of 0.5 MeV, then this causes water to emit a bluish white light usually referred to as Čerenkov light. It is possible to detect this light using a typical liquid scintillation counter.

Since there is no requirement for organic solvents and fluors, this technique is relatively cheap, sample preparation is very easy, and there is no problem of chemical quenching. Table 14.6 lists some isotopes that are suitable for this detection method. Most work has been done on  $^{32}\text{P}$ , which has 80% of its energy spectrum above the Čerenkov threshold and which can be detected at around 40% efficiency. It may be noted from Table 14.6 that, as the proportion of the energy spectrum above 0.5 MeV increases, so too does the detection efficiency.

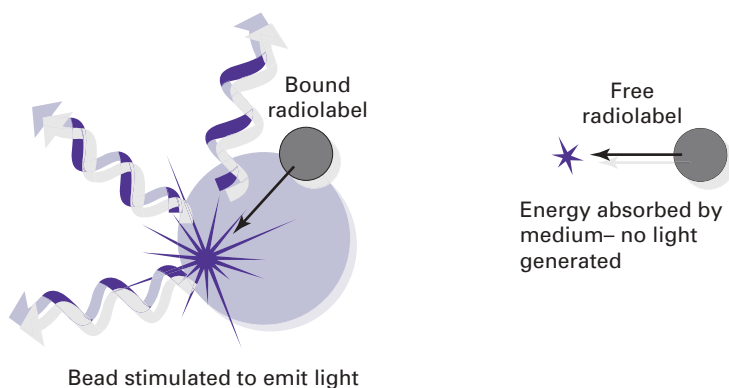


Fig. 14.12. The concept behind SPA. (Reproduced by courtesy of Amersham Biosciences.)

**Table 14.7 Advantages of scintillation proximity assay**

Versatile: use with enzyme assays, receptors, any molecular interactions  
 Works with a range of appropriate isotopes such as  $^3\text{H}$ ,  $^{14}\text{C}$ ,  $^{35}\text{S}$  and  $^{33}\text{P}$   
 No need for separation step (e.g. free from bound ligand)  
 Less manipulation therefore reduced toxicity  
 Amenable to automation

**Scintillation proximity assay**

Scintillation proximity assay (SPA) is an application of scintillation counting that facilitates automation and rapid throughput of experiments. It is therefore highly suited to work such as screening for biological activity in new drugs. The principle of SPA is illustrated in Fig. 14.12. SPA beads are constructed from polystyrene (or sometimes other materials) that combine a binding site for a molecule of interest with a scintillant. You need to remember that some types of radiation do not travel far, in particular  $\beta$ -particles from weak energy emitters such as  $^3\text{H}$  and  $^{14}\text{C}$ . If molecules containing such radioisotopes are in solution with a suspension of SPA beads, the radiation does not stimulate the scintillant in the beads and cannot be detected efficiently by a scintillation counter. This is because the radiation is absorbed by the solution; it does not reach the scintillant. If, on the other hand, the radioisotope becomes bound to the bead, it is close enough to stimulate the scintillant in the bead, so light is given out and the isotope is detected.

There are many applications of this technology such as enzyme assays and receptor binding, indeed any situation where we want to investigate the interaction between two molecules. Take receptor binding as an example. In this case a receptor for a particular ligand (such as a drug or hormone) is attached to the SPA beads. The ligand is radiolabelled and mixed with the beads. Any ligand that binds will stimulate the scintillant and be counted. If the researcher wishes to investigate chemicals that might interface with this binding (which is the mode of action

of many medicines), they can be added at increasing concentration to study the effect and, for example, determine optimum dosage (see also Section 16.3.2).

A summary of the advantages of SPA technology is shown in Table 14.7.

### 14.2.3 Methods based upon exposure of photographic emulsions

Ionising radiation acts upon a photographic emulsion to produce a latent image much as does visible light. For a photograph, a radiation source, an object to be imaged and photographic emulsion are required. For an autoradiograph, a radiation source (i.e. radioactivity) emanating from within the material to be imaged (the object) is required, along with a sensitive emulsion. The emulsion consists of a large number of silver halide crystals embedded in a solid phase such as gelatin. As energy from the radioactive material is dissipated in the emulsion, the silver halide becomes negatively charged and is reduced to metallic silver, thus forming a particulate latent image. Photographic developers are designed to show these silver grains as a blackening of the film, and fixers remove any remaining silver halide. Thus a permanent image of the location of the original radioactive event remains.

This process, which is known as *autoradiography*, is very sensitive and has been used in a wide variety of biological experiments. These unusually involve a requirement to locate the distribution of radioactivity in biological specimens of different types. For instance, the sites of localisation of a radiolabelled drug throughout the body of an experimental animal can be determined by placing whole-body sections of the animal in close contact with a sensitive emulsion such as an X-ray plate. After a period of exposure, the plate, upon development, will show an image of the section in tissues and organs in which radioactivity was present. Similarly, radioactive metabolites isolated and separated by chromatographic or electrophoretic techniques during metabolic studies can be located on the chromatograph or electrophoretograph and the radioactive spots can subsequently be recovered for counting and identification.

The techniques of autoradiography (Fig. 14.13) have become more important with recent developments in molecular biology (Chapters 5 and 6). Consequently more detail is given below on some important aspects of the technique.

#### Suitable isotopes

In general, weak  $\beta$ -emitting isotopes (e.g.  $^3\text{H}$ ,  $^{14}\text{C}$  and  $^{35}\text{S}$ ) are most suitable for autoradiography, particularly for cell and tissue localisation experiments. This is because, as a result of the low energy of the negatrons, the ionising track of the isotope will be short and a discrete image will result. This is particularly important when radioactivity associated with subcellular organelles is being located. For this,  $^3\text{H}$  is the best radioisotope, since its energy will all be quickly dissipated within the emulsion. Electron microscopy can then be used to locate the image in the developed film. For location within whole organisms or tissues, either  $^{14}\text{C}$  or  $^3\text{H}$  is suitable; more energetic isotopes (e.g.  $^{32}\text{P}$ ) are less suitable because their higher energy negatrons produce much longer track lengths and result in less

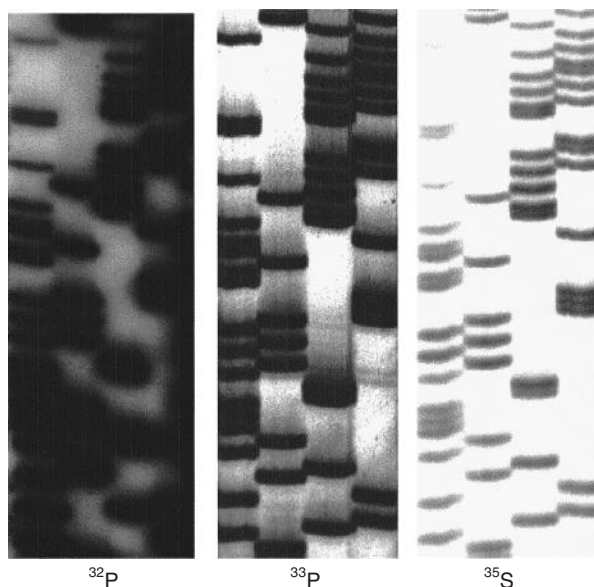


**Fig. 14.13.** Three autoradiograph showing the use of different radioisotopes in DNA sequencing. The isotope with the highest energy ( $^{32}\text{P}$ ) leads to the poorest resolution because the radiation spreads out further, making the DNA bands appear thicker. The lowest energy radiation (from  $^{35}\text{S}$ ) gives the best resolution. (Reproduced with permission from M. W. Cunningham, A. Patel, A. C. Simmonds and D. Williams (2002), *In vitro* labelling of nucleic acids and proteins, in *Radioisotopes in Biology*, (2nd edn), R. J. Slaten (ed.), Oxford University Press, Oxford.)

discrete images that are not sufficiently discriminatory for microscopic location. Conversely, for location of, for example, DNA bands in an electrophoretic gel,  $^{32}\text{P}$  is useful. In this case low energy  $^3\text{H}$  neutrons would largely dissipate their energy within the gel (and in the wrapping around the gel, which is usually necessary to prevent the gel sticking to the emulsion), thereby reducing sensitivity to a low level. However, the more energetic  $^{32}\text{P}$  neutrons will leave the gel and produce a strong image. If very thin gels are prepared, then  $^{35}\text{S}$  or  $^{14}\text{C}$  can be detected with high resolution, for example in DNA sequencing gels where  $^{35}\text{S}$  is used as the label.

#### Choice of emulsion and film

A variety of emulsions is available with different packing densities of the silver halide crystals. Care must be taken to choose an emulsion suitable for the purposes of the experiment, since the sensitivity of the emulsion will affect the resolution obtained. Manufacturers' literature should be consulted and their advice sought if one is in any doubt. X-ray film is generally suitable for macroscopic samples such as whole-body sections of small mammals, chromatographs or electrophoretographs. When light or electron microscopic detection of the location



of the image in the emulsion is required (cellular and subcellular localisation of radioactivity), very sensitive films are necessary, as is a very close apposition of sample and film. In these cases a **stripping film technique** can be used in which the film is supplied attached to a support. It is stripped from this and applied directly to the sample. Alternatively, liquid emulsions are prepared by melting strips of emulsion by heating them to around 60°C. Then either the emulsion is poured onto the sample or the sample attached to a support is dipped into the emulsion. The emulsion is then allowed to set before being dried. Such a method is often referred to as a **dipping-film method** and is preferred when very thin films are required.

### Background

Accidental exposure to light, chemicals in the sample, natural background radioactivity (particularly  $^{40}\text{K}$  in glass) and even pressure applied during handling and storage of film will cause a background fog (i.e. latent image) on the developed film. This can be problematic, particularly in high resolution work (e.g. involving microscopy) and care must be taken at all times to minimise its effect. Background will always increase during exposure time, which should therefore always be kept to a minimum.

### Time of exposure and film processing

The time of exposure depends upon the isotope, sample type, level of activity, film type and purpose of the experiment. The same applies to the processing of the film in order to display the image. Generally the process must be adapted to a given purpose, and a great deal of trial and error is often involved in arriving at the most suitable procedures.

### Direct autoradiography

In direct autoradiography, the X-ray film or emulsion is placed as close as possible to the sample and exposed at any convenient temperature. Quantitative images are produced until saturation is reached. The approach provides high resolution but limited sensitivity: isotopes of energy equal to, or higher than,  $^{14}\text{C}$  ( $E_{\text{max}} = 0.156 \text{ MeV}$ ) are required.

### Fluorography

Many of the currently popular methods in molecular biology involve separation of macromolecules or fractions of macromolecules by gel electrophoresis (Sections 10.3 and 10.4). The separated macromolecules or fractions form bands in the electrophoretograph that must be located. This is often achieved by radiolabelling the macromolecules with  $^3\text{H}$  or  $^{14}\text{C}$  and subjecting the gel to autoradiography. Because these are weak  $\beta$ -emitters, much of their energy is lost in the gel and long exposure times are necessary even when very high specific activity sources are used. However, if a fluor (e.g. PPO or sodium silicate) is infiltrated into the gel, and the gel dried and then placed in contact with a preflashed film (see below), sensitivity can be increased by several orders of magnitude. This is

because the negatrons emitted from the isotope will cause the fluor to become excited and emit light, which will react with the film. Thus use is made of both the ionising and the exciting effects of radioactivity in fluorography.

### Intensifying screens

When  $^{32}\text{P}$ -labelled or  $\gamma$ -isotope-labelled samples (e.g.  $^{32}\text{P}$ ] DNA or  $^{125}\text{I}$ -labelled protein fractions in gels) are to be located, the opposite problem to that presented by low energy isotopes prevails. These much more penetrating particles and rays cause little reaction with the film as they penetrate right through it, producing a poor image. The image can be greatly improved by placing, on the other side of the film from the sample, a thick **intensifying screen** consisting of a solid phosphor. Negatrons penetrating the film cause the phosphor to fluoresce and emit light, which superimposes its image on the film. There is, therefore, an increase in sensitivity but a parallel reduction in resolution due to the spread of light emanating from the screen.

### Low temperature exposure

If the energy of ionising radiation is converted to light (i.e. with fluorography or intensifying screens) the kinetics of the film's response are affected. The light is of low intensity and a back reaction occurs that cancels the forming latent image. Exposure at low temperature ( $-70^\circ\text{C}$ ) slows this back reaction and will therefore provide higher sensitivity. There is no point in doing direct autoradiography at low temperature as the kinetics of the film response are different. There is nothing to be gained by exposing preflashed film (see below) at low temperature.

### Preflashing

As described above, the response of a photographic emulsion to radiation is not linear and usually involves a slow initial phase (lag) followed by a linear phase. Sensitivity of films may be increased by **preflashing**. This involves a millisecond light flash prior to the sample being brought into juxtaposition with the film and is often used where high sensitivity is required or if results are to be quantified.

### Quantification

As indicated earlier, autoradiography is usually used to locate rather than to quantify radioactivity. However, it is possible to obtain quantitative data directly from autoradiographs by using a densitometer, which records the intensity of the image. This in turn is related to the amount of radioactivity in the original sample. There are many varieties of densitometers available and the choice made will depend on the purpose of the experiment. Quantification is not reliable at low or high levels of exposure because of the lag phase (i.e. the back reaction, as described above) or saturation, respectively; however, preflashing combined with fluorography or intensifying screens obviates the problem for small amounts of radioactivity. In this case all photons contribute equally to the image of the pre-exposed film.

### 14.3 OTHER PRACTICAL ASPECTS OF COUNTING RADIOACTIVITY AND ANALYSIS OF DATA

#### 14.3.1 Counter characteristics

##### Background count

Radiation counters of all types always register a count, even in the absence of radioactive material in the apparatus. This may be due to such sources as cosmic radiation, natural radioactivity in the vicinity, nearby X-ray generators, and/or circuit noises. By means of the various methods already outlined and the use of lead shielding, this **background radiation** may be considerably reduced, but its value must always be recorded and accounted for in all experiments. Some commercial instruments have automatic background subtraction facilities.

##### Dead time

At very high count rates in Geiger–Müller counting, counts are lost due to the dead time of the Geiger–Müller tube. Correction tables are available and these should be used when necessary to correct for lost counts. Dead time is not a problem in scintillation counting.

##### Geometry

When samples with an end-window ionisation counter, such as a Geiger–Müller tube, are compared, it is important to standardise the position of the sample in relation to the tube, otherwise the fraction of the emitted radiation entering the tube may vary and hence so will the observed count.

#### 14.3.2 Sample and isotope characteristics

##### Self-absorption

Self-absorption is primarily a problem with low energy  $\beta$ -emitters: radiation is absorbed by the sample itself. Self-absorption can be a serious problem in the counting of low energy radioactivity by scintillation counting if the sample is particulate or is, for instance, stuck to a membrane filter. Care should be taken to ensure comparability of samples because the methods of standardisation outlined earlier will not correct for self-absorption effects. Where homogeneity is not possible, particulate samples should be digested or otherwise solubilised prior to counting. Self-absorption is a major problem with Geiger–Müller counting and significantly reduces sensitivity and reliability. It is very difficult to count low energy emitters reliably with these counters and this was a major factor in the switch to scintillation counting.

##### Half-life

The half-life of an isotope (Section 14.1.5) may be short and, if so, this must be allowed for in the analysis of data.

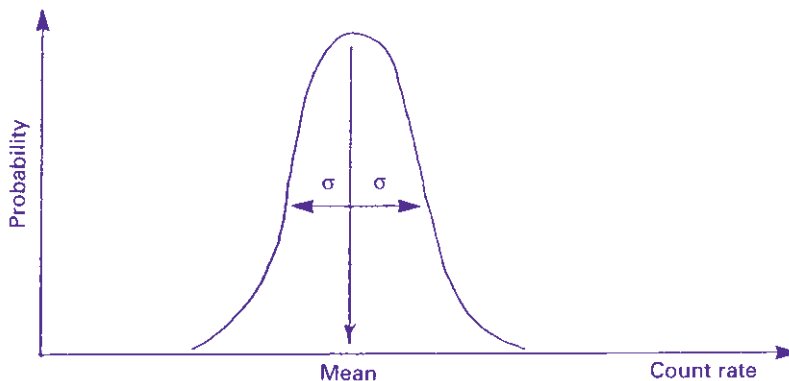


Fig. 14.14. The distribution of count rates around a mean, showing the standard deviation,  $\sigma$ .

### Statistics

The emission of radioactivity is a random process. This can be demonstrated readily by making repeated measurements of the activity of a long-lived isotope, each for an identical period of time. The resulting counts will not be the same but will vary over a range of values, with clustering near the centre of the range. If a sufficiently large number of such measurements is made and the data are plotted, a normal distribution curve will be obtained. For a single count, therefore, we cannot obtain a true count. Instead, we take the mean of a large number of counts as being very close to the true count. However, the accuracy of this mean will depend on the spread or standard deviation ( $\sigma$ ) for the data. Statistical theory states that, for a normal distribution such as that shown in Fig. 14.14, 68.2% of values obtained lie  $\pm 1 \sigma$ , and 95.5% lie  $\pm 2 \sigma$  from the mean ( $\bar{x}$ ) (Section 1.6.3).

Clearly, if we wish to compare samples, and in particular to state that two samples contain different amounts of radioactivity, then we need to take account of the counting statistics. Fortunately Poisson mathematics makes the task relatively easy as

$$\sigma = \sqrt{\text{total counts taken}} \quad (14.7a)$$

or

$$\sigma = \sqrt{\left(\frac{\text{count rate}}{\text{time}}\right)} \quad (14.7b)$$

Therefore to quote a figure with 95.5% certainty, state:

$$\text{total counts} \pm 2 \sqrt{\text{total counts}} \quad (14.8)$$

For example, if 1600 counts are recorded this can be expressed as  $1600 \pm 80$ . There is, therefore, a 95.5% chance that the true figure lies between 1520 and 1680.

When data are expressed as d.p.m. or c.p.m., again using 95.5% certainty, then

$$\text{error on count rate} = 2 \sqrt{\left(\frac{\text{count rate}}{\text{time}}\right)} \quad (14.9)$$

Using the same example, if the 1600 counts were obtained in 1 min:

$$\text{error on count rate} = 2 \sqrt{\left(\frac{1600}{1}\right)} = 80$$

and therefore 1600 c.p.m.  $\pm$  80 c.p.m.

If the 1600 counts were obtained in 10 min:

$$\text{error on count rate} = 2 \sqrt{\left(\frac{160}{10}\right)} = 8$$

and therefore 160 c.p.m.  $\pm$  8 c.p.m. Note that the error is the same. This is because effectively the same number of measurements, i.e. counts, has been taken in each case.

If we had recorded 160 counts in only 1 min, then:

$$\text{error on count rate} = 2 \sqrt{\left(\frac{160}{1}\right)} = 25$$

and therefore 160 c.p.m.  $\pm$  25 c.p.m.

Consider these other simple examples for a series of 1 min counts:

$$\begin{array}{lll} \text{counts} = 100 & \sigma = \sqrt{100}, & \text{therefore } \pm 10\% \text{ error at } 68.2\% \text{ certainty} \\ \text{counts} = 1000 & \sigma = \sqrt{1000}, & \text{therefore } \pm 3\% \text{ error at } 68.2\% \text{ certainty} \\ \text{counts} = 10\,000 & \sigma = \sqrt{10\,000}, & \text{therefore } \pm 1\% \text{ error at } 68.2\% \text{ certainty} \end{array}$$

In summary, the counts per minute data become more accurate for *higher count rates* and/or *longer counting times*. It is common practice to count to 10 000 counts or for 10 min, whichever is the quicker, although for very low count rates longer counting times are required.

### Example 6 ACCURACY OF COUNTING

#### Question

A sample recording 564 c.p.m. was counted over 10 min. What is the accuracy of the measurement for 95.5% confidence?

#### Answer

It is necessary to apply equation 14.9 to calculate the counting error:

$$\text{counting error} = 2\sqrt{564/10} = 15$$

so the range in which the counts should fall with 95.5% confidence is  $564 \pm 15$ .

#### 14.3.3 Supply, storage and purity of radiolabelled compounds

There are several suppliers of radiolabelled compounds, the main ones being Amersham Biosciences plc., Du Pont, NEN and ICN. The suppliers usually include

details of the best storage conditions and quality control data with their products. This is because several types of decomposition can occur; for example internal decomposition resulting from radioactive decay such as  $^{14}\text{C} \rightarrow ^{14}\text{N}$ , and external decomposition where emitted radiation is absorbed by other radioactive molecules, causing impurities. The extent to which decomposition occurs is dependent on many factors such as temperature, energy of radiation, concentration and the formulation of the compound. It is, therefore, imperative to store radioisotopes by the method recommended by the supplier and to maintain sterility of the stock. If necessary, chromatographic procedures will be required to check on the purity of the labelled compounds.

#### 14.3.4 Specific activity

The specific activity of a radioisotope defines its radioactivity related to the amount of material (e.g.  $\text{Bq mol}^{-1}$ ,  $\text{Ci mmol}^{-1}$  or d.p.m.  $\mu\text{mol}^{-1}$ ). Suppliers offer a range of specific activities for their compound, the highest often being the most expensive. The advantages of using a very high specific activity are as follows:

- Products of a reaction using the labelled precursor can be produced at high specific activity (e.g. for DNA probes, see Section 5.10).
- Small quantities of radiolabelled compound can be added such that the equilibrium of metabolic concentrations is not unduly perturbed.
- Calculating the amount of substance required to make up radioactive solutions of known specific activity is simplified, as the contribution to concentration made by the stock radiolabelled solution is often negligible (see below).

Sometimes, however, it is not necessary to purchase the highest specific activity available. For example, enzyme assays *in vitro* often require a relatively high substrate concentration and so specific activity may need to be lowered. Consider the example below (for definitions of units, see Table 14.10):

$^3\text{H}$ Leucine is purchased with a specific activity of  $5.55 \text{ TBq mmol}^{-1}$  ( $150 \text{ Ci mmol}^{-1}$ ) and a concentration of  $9.25 \text{ MBq } 250 \text{ mm}^{-3}$  ( $250 \mu\text{Ci } 250 \text{ mm}^{-3}$ ). A  $10 \text{ cm}^3$  solution of  $250 \text{ mM}$  and  $3.7 \text{ kBq cm}^{-3}$  ( $0.1 \mu\text{Ci cm}^{-3}$ ) is required. It is made up as follows:

- $10 \text{ cm}^3$  at  $3.7 \text{ kBq cm}^{-3}$  is  $37 \text{ kBq}$  ( $1 \mu\text{Ci}$ ), therefore pipette  $1 \text{ mm}^3$  of stock radioisotope into a vessel (or, to be more accurate, pipette  $100 \text{ mm}^3$  of a  $\times 100$  dilution of stock in water).
- Add  $2.5 \text{ cm}^3$  of a  $1 \text{ M}$  stock solution of cold leucine, and make up to  $10 \text{ cm}^3$  with distilled water.

There is no need to take into account the amount of unlabelled leucine in the  $^3\text{H}$ leucine preparation; it is a negligible quantity due to the high specific activity. If necessary (e.g. to manipulate solutions of relatively low specific activity), however, the following formula can be applied:

$$W = Ma[(1/A') - (1/A)] \quad (14.10)$$

where  $W$  is the mass of cold carrier required (mg),  $M$  is the amount of radioactivity present (MBq),  $a$  is the molecular weight of the compound,  $A$  is the original specific activity (MBq mmol<sup>-1</sup>), and  $A'$  is the required specific activity (MBq mmol<sup>-1</sup>).

### Example 7 MAKING UP A SOLUTION OF KNOWN ACTIVITY

#### Question

One litre of [<sup>3</sup>H]uridine with a concentration of 100 μmol cm<sup>-3</sup> and 50 000 c.p.m. cm<sup>-3</sup> is required. If all measurements are made on a scintillation counter with an efficiency of 40%, how would you make up this solution if the purchased supply of [<sup>3</sup>H]uridine has a specific activity of 20/Ci mol<sup>-1</sup>?

[NB:  $M_r$  uridine = 244; 1 Ci =  $22.2 \times 10^{11}$  d.p.m.]

Repeat the calculation in becquerels.

#### Answer

This problem is similar to the leucine example given above. Correcting for the 48% counting efficiency: 50 000 c.p.m. is 125 000 d.p.m. Multiplying this by 10<sup>3</sup> for a litre gives a d.p.m. equivalent of 56.3 μCi ( $125 \times 10^6 / 22.2 \times 10^5 = 56.3 \mu\text{Ci}$ ). Given 20 Ci mol<sup>-1</sup>, work out how many moles there are in 56.3 μCi ( $56.3 / 20 \times 10^6 = 2.815 \mu\text{moles}$ ). 100 000 μmoles of uridine are required in a litre; from the molecular mass this is 24.4 g. The 2.815 μmoles from the radioactive input is only 0.685 mg and so can effectively be ignored. The answer is, therefore, 56.3 μCi (2.08 MBq) of [<sup>3</sup>H]uridine plus 24.4 g of uridine.

#### 14.3.5 The choice of radionuclide

This is a complex question depending on the precise requirements of the experiment. A summary of some of the key features of radioisotopes commonly used in biological work is shown in Table 14.8.

#### 14.4 INHERENT ADVANTAGES AND RESTRICTIONS OF RADIOTRACER EXPERIMENTS

Perhaps the greatest advantage of radiotracer methods over most other chemical and physical methods is their sensitivity. For example, a dilution factor of 10<sup>12</sup> can be tolerated without the detection of <sup>3</sup>H-labelled compounds being jeopardised. It is thus possible to detect the occurrence of metabolic substances that are normally present in tissues at such low concentrations as to defy the most sensitive chemical methods of identification. A second major advantage of using radiotracers is that they enable studies *in vivo* to be carried out to a far greater degree than can any other technique.

In spite of these significant advantages, certain restrictions have to be appreciated. First, although they undergo the same reactions, different isotopes may do so at different rates. This effect is known as the **isotope effect**. The different rates are approximately proportional to the differences in mass between the isotopes. The extreme case is the isotopes <sup>1</sup>H and <sup>3</sup>H, the effect being small for <sup>12</sup>C and <sup>14</sup>C and

**Table 14.8** The relative merits of commonly used  $\beta$ -emitters

Isotope	Advantages	Disadvantages
$^3\text{H}$	Safety High specific activity possible Wide choice of positions in organic compounds Very high resolution in autoradiography	Low efficiency of detection Isotope exchange with environment Isotope effect
$^{14}\text{C}$	Safety Wide choice of labelling position in organic compounds Good resolution in autoradiography	Low specific activity
$^{35}\text{S}$	High specific activity Good resolution in autoradiography	Short half-life Relatively long biological half-life
$^{33}\text{P}$	High specific activity  Good resolution in autoradiography Less hazardous than $^{32}\text{P}$	Lower specific activity than $^{32}\text{P}$ Less sensitive than $^{32}\text{P}$ Cost
$^{32}\text{P}$	Ease of detection High specific activity  Short half-life simplifies disposal Čerenkov counting	Short half-life affects costs and experimental design External radiation hazard  Poor resolution in autoradiography

Taken from *Radioisotopes in Biology, A Practical Approach*, 2nd edn, ed. R. J. Slater (2002), Oxford University Press, with permission.

almost insignificant for  $^{33}\text{P}$  and  $^{32}\text{P}$ . Secondly, the amount of activity employed must be kept to the minimum necessary to permit reasonable counting rates in the samples to be analysed, otherwise the radiation from the tracer may elicit a response from the experimental organism and hence distort the results. A third consideration is that, in order to administer the tracer, the normal chemical level of the compound in the organism is automatically exceeded. The results are therefore always open to question.

#### 14.5 SAFETY ASPECTS

The greatest practical disadvantages of using radioisotopes is their toxicity: they produce ionising radiations. When absorbed, radiation causes ionisation and free



radicals form that interact with the cell's macromolecules, causing mutation of DNA and hydrolysis of proteins. The toxicity of radiation is dependent not simply on the amount present but on the amount absorbed by the body, the energy of the absorbed radiation and its biological effect. There are, therefore, a series of additional units used to describe these parameters. Originally, radiation hazard was measured in terms of **exposure**, i.e. a quantity expressing the amount of ionisation in air. The unit of exposure is the **roentgen** (R), which is the amount of radiation that produces  $1.61 \times 10^{15}$  ion-pairs  $(\text{kg air})^{-1}$  (or  $2.58 \times 10^{-4}$  coulombs  $(\text{kg air})^{-1}$ ).

The amount of energy required to produce an ion-pair in air is  $5.4 \times 10^{-18}$  joules (J) and so the amount of energy absorbed by air with an exposure of 1 R is:

$$1.61 \times 10^{15} \times 5.4 \times 10^{-18} = 0.00869 \text{ J (kg air)}^{-1}$$

Although the roentgen has been used as a unit of radiation hazard, it is now considered inadequate for two reasons: first, it is defined with reference to X-rays (or  $\gamma$ -rays) only; and, secondly, the amount of ionisation or energy absorption in different types of material, including living tissue, is likely to be different from that in air.

The concept of **radiation absorbed dose** (rad) was introduced to overcome these restrictions. The rad is defined as the dose of radiation that gives an energy absorption of  $0.01 \text{ J (kg absorber)}^{-1}$ ; this has now been changed to the gray, an SI unit, representing absorption of  $1 \text{ J kg}^{-1}$  (i.e. 100 rads).

The **gray** (Gy) is a useful unit, but it still does not adequately describe the hazard to living organisms. This is because different types of radiation are associated with differing degrees of biological hazard. It is, therefore, necessary to introduce a correction factor, known as the **weighting factor** ( $W$ ), which is calculated by comparing the biological effects of any type of radiation with that of X-rays. The unit of absorbed dose, which takes into account the weighting factor is the **sievert** (Sv) and is known as the **equivalent dose**. Thus:

$$\text{equivalent dose (Sv)} = \text{Gy} \times W \quad (14.11)$$

The majority of isotopes used in biological research emit  $\beta$ -radiation. This is considered to have a biological effect that is very similar to X-rays and has a weighting factor of 1. Therefore, for  $\beta$ -radiation,  $\text{Gy} = \text{Sv}$ . Alpha particles, with their stronger ionising power, are much more toxic and have a weighting factor of 20. Therefore, for  $\alpha$ -radiation,  $1 \text{ Gy} = 20 \text{ Sv}$ . It is likely that, as our knowledge of the biological effectiveness of different forms of radiation progresses, so the quality factor for different types of radiation may change in the future. Absorbed dose from known sources can be calculated from knowledge of the rate of decay of the source, the energy of radiation, the penetrating power of the radiation and the distance between the source and the laboratory worker. As the radiation is emitted from a source in all directions, the level of irradiation is related to the area of a sphere,  $4\pi r^2$ . Thus the absorbed dose is inversely related to the square of the distance from the source ( $r$ ); or, put another way, if the distance is doubled the dose is quartered. A useful formula is

$$\text{dose}_1 \times \text{distance}_1^2 = \text{dose}_2 \times \text{distance}_2^2 \quad (14.12)$$

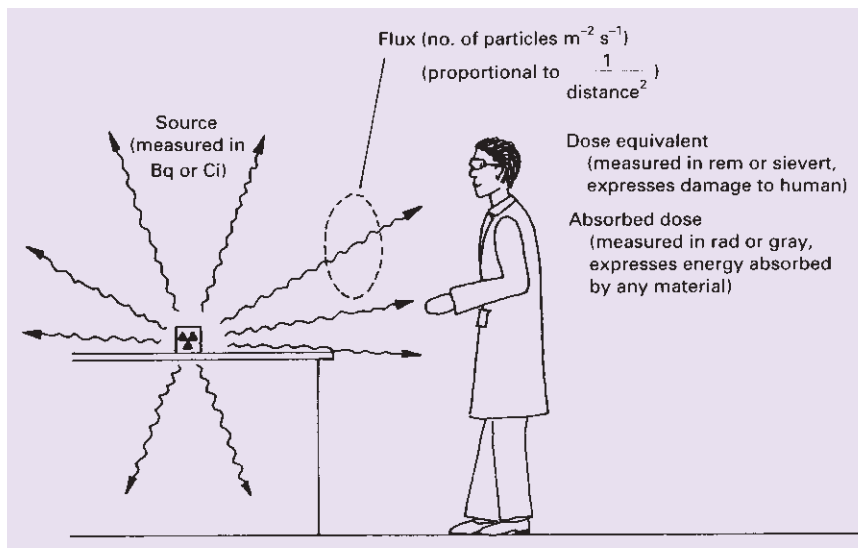


Fig. 14.15. The relationship between radioactivity of source and absorbed dose.

The relationship between radioactive source and absorbed dose is illustrated in Fig. 14.15.

The rate at which dose is delivered is referred to as the **dose rate**, expressed in  $Sv\ h^{-1}$ . It can be used to calculate your **total dose**. For example, a source may be delivering  $10\ \mu Sv\ h^{-1}$ . If you worked with the source for 6 h, your total dose would be  $60\ \mu Sv$ .

Currently the dose limit for workers exposed to radiation is 15 mSv in a year to the whole body, but this is rarely ever approached by biologists because the levels of radiation used are so low. Limits are set for individual organs. The most important of these to know are for hands ( $500\ mSv\ year^{-1}$ ) and for lens of the eye ( $150\ mSv\ year^{-1}$ ). Dose limits are constantly under review and, although dose limits are set, it is against internationally agreed guidelines to work to such a limit, i.e. to assume that all is satisfactory if the limit is not exceeded. Instead, the ALARA principle is applied, to work always to a dose limit that is as low as reasonably achievable. Work that may cause a worker to exceed three-tenths or one-tenth of the dose limit must be carried out in a controlled area or a supervised area, respectively. In practice, work in the biosciences rarely involves a worker receiving a measurable dose. Supervised areas are common but not always required (e.g. for  $^3H$  or  $^{14}C$  experiment). Controlled areas are required in only certain circumstances, for example for isotope stores or radioiodination work. A major problem, however, in biosciences is the **internal radiation hazard**. This is caused by radiation entering the body, for example by inhalation, ingestion, absorption or puncture. This is a likely source of hazard where work involves **open sources**, i.e. liquids and gases; most work in biology involves manipulations of radioactive liquids. Control of contamination is assisted by:

**Table 14.9** Annual limits on intake (ALI) for some commonly used isotopes

Nuclide	ALI (MBq)
$^3\text{H}$	480
$^{14}\text{C}$	34
$^{32}\text{P}$	6.3
$^{125}\text{I}$	1.3

- complying with local rules, written by an employer,
- conscientious personal conduct in the laboratory,
- regular monitoring,
- carrying out work in some kind of containment.

Calculating the dose received following the ingestion of a radioisotope is complex. Detailed information is published by the International Commission on Radiological Protection and assessments, for example for experiments on human volunteers, can be obtained from the National Radiological Protection Board. However, one relatively simple concept is the **annual limit on intake (ALI)**. The ingestion of one ALI results in a person receiving a dose limit to the whole body or to a particular organ. Some ALIs are shown in Table 14.9. Management of radiation protection is similar in most countries. In the USA, there is a **Code of Federal Regulations**. In the UK there is the **Radioactive Substances Act (1993)** and the **Ionising Radiations Regulations (1999)**. Every institution requires certification (monitored by the Environmental Protection Agency in the USA or the Environment Agency in the UK) and employs a Radiation Protection Advisor.

When handling radioisotopes the rule is to:

- maximise the distance between yourself and the source,
- minimise the time of exposure and
- maintain shielding at all times.

## 14.6 APPLICATIONS OF RADIOISOTOPES IN THE BIOLOGICAL SCIENCES

### 14.6.1 Investigating aspects of metabolism

#### Metabolic pathways

Radioisotopes are frequently used for tracing metabolic pathways. This usually involves adding a radioactive substrate, taking samples of the experimental material at various times, extracting and chromatographically, or otherwise, separating the products. Radioactivity detectors can be attached to gas-liquid chromatography or high performance liquid chromatography columns to monitor radioactivity coming off the column during separation. Alternatively, radioactivity can be located on paper or thin-layer chromatography with either a

Geiger–Müller chromatograph scanner or with autoradiography. If it is suspected that a particular compound is metabolised by a particular pathway, then radioisotopes can also be used to confirm this. For instance, it is possible to predict the fate of individual carbon atoms of [ $^{14}\text{C}$ ]acetate through the tricarboxylic acid, or Krebs, cycle. Methods have been developed whereby intermediates of the cycle can be isolated and the distribution of carbon within each intermediate can be ascertained. This is the so-called **specific labelling pattern**. Should the actual pattern coincide with the theoretical pattern, then this is very good evidence for the mode of operation of the Krebs cycle.

Another example of the use of radioisotopes to confirm the mode of operation, or otherwise, of a metabolic pathway is in studies carried out on glucose catabolism. There are numerous ways whereby glucose can be oxidised, the two most important ones in aerobic organisms being glycolysis followed by the Krebs cycle together with the pentose phosphate pathway. Frequently, organisms or tissues possess the necessary enzymes for both pathways to occur and it is of interest to establish the relative contribution of each to glucose oxidation. Both pathways involve the complete oxidation of glucose to carbon dioxide, but the origin of the carbon dioxide in terms of the six carbon atoms of glucose is different (at least in the initial stages of respiration of exogenously added substrate). Thus it is possible to trap the carbon dioxide evolved during the respiration of specifically labelled glucose (e.g. [ $6\text{-}^{14}\text{C}$ ]glucose or [ $1\text{-}^{14}\text{C}$ ]glucose in which only the C-6 atom is radioactive) and obtain an evaluation of the contribution of each pathway to glucose oxidation.

The use of radioisotopes in studying the operation of the Krebs cycle or in evaluating the pathway of glucose catabolism are just two examples of how such isotopes can be used to confirm metabolic pathways. Further details of these and other examples, including use of dual-labelling methods, can be found in the various texts recommended in Section 14.7.

### **Metabolic turnover times**

Radioisotopes provide a convenient method of ascertaining turnover times for particular compounds. As an example, the turnover of proteins in rats will be considered. A group of rats is injected with a radioactive amino acid and left for 24 h, during which time most of the amino acid is assimilated into proteins. The rats are then killed at suitable time intervals and radioactivity in organs or tissues of interest is determined. In this way it is possible to ascertain the rate of metabolic turnover of protein. Using this sort of method, it has been shown that liver protein is turned over in 7–14 days, while skin and muscle protein is turned over every 8–12 weeks, and collagen is turned over at a rate of less than 10% per annum.

### **Studies of absorption, accumulation and translocation**

Radioisotopes have been very widely used in the study of the mechanisms and rates of absorption, accumulation and translocation of inorganic and organic compounds by both plants and animals. Such experiments are generally simple to

perform and can also yield evidence on the route of translocation and sites of accumulation of molecules of biological interest.

### Pharmacological studies

Another field where radioisotopes are widely used is in the development of new drugs. This is a particularly complicated process, because, besides showing whether a drug has a desirable effect, much more must be ascertained before it can be used in the treatment of clinical conditions. For instance, the site of drug accumulation, the rate of accumulation, the rate of metabolism and the metabolic products must all be determined. In each of these areas of study, radiotracers are extremely useful, if not indispensable. For instance, autoradiography on whole sections of experimental animals (Section 14.2.3) yields information on the site and rate of accumulation, while typical techniques used in metabolic studies can be used to follow the rate and products of metabolism.

## 14.6.2 Analytical applications

### Enzyme and ligand binding studies

Virtually any enzyme reaction can be assayed using radiotracer methods, as outlined in Section 15.2.2, provided that a radioactive form of the substrate is available. Radiotracer-based enzyme assays are more expensive than other methods, but frequently have the advantage of a higher degree of sensitivity. Radioisotopes have also been used in the study of the mechanism of enzyme action and in studies of ligand binding to membrane receptors (Section 16.3.1).

### Isotope dilution analysis

There are many compounds present in living organisms that cannot be accurately assayed by conventional means because they are present in such low amounts and in mixtures of similar compounds. Isotope dilution analysis offers a convenient and accurate way of overcoming this problem and avoids the necessity of quantitative isolation. For instance, if the amount of iron in a protein preparation is to be determined, this may be difficult using normal methods, but it can be done if a source of  $^{59}\text{Fe}$  is available. This is mixed with the protein and a sample of iron is subsequently isolated, assayed for total iron and the radioactivity determined.

If the original specific activity was  $10\,000\text{ d.p.m. (10 mg)}^{-1}$  and the specific activity of the isolated iron was  $9000\text{ d.p.m. (10 mg)}^{-1}$  then the difference is due to the iron in the protein ( $x$ ), i.e.

$$\frac{9000}{10} = \frac{10\,000}{10 + x} \quad (14.13)$$

therefore  $x = 1.1\text{ mg}$ .

This technique is widely used in, for instance, studies on trace elements.

**Example 8 ISOTOPE DILUTION CALCULATION****Question**

To determine the nutritional quality of protein in a foodstuff the content of lysine was determined by isotope dilution analysis. To an acid hydrolysate of the protein (1 mg), 0.5  $\mu\text{mole}$  of [ $^3\text{H}$ ]lysine ( $1 \text{ Ci mol}^{-1}$ ) was added. A sample of lysine was purified from the hydrolysate by chromatography and the specific activity determined by scintillation counting at 25% efficiency. The value obtained was 2071 c.p.m.  $\mu\text{g}^{-1}$ . What is the % (w/w) lysine content of soybean protein?  $1 \text{ Ci} = 22.2 \times 10^{11} \text{ d.p.m.}$ ;  $M_r \text{ lysine} = 148$ .

**Answer**

To address this problem it is necessary to apply equation 14.13. Since the counting efficiency was only 25%, it is necessary to multiply the observed count by 4.

0.5  $\mu\text{mole}$  of lysine = 74  $\mu\text{g}$ . Hence, using equation 14.13, we get:

$$(2071 \times 4)/1 = (22.2 \times 10^{11} \times 0.5 \times 10^{-6}) / (74 + x)$$

where  $x$  is the lysine content of the sample. From this equation,  $x = 60 \mu\text{g}$  or 6% of the 1 mg protein sample.

**Radioimmunoassay**

One of the most significant advances in biochemical techniques in recent years has been the development of the radioimmunoassay. This technique is discussed in Section 7.7 and is not elaborated upon here.

**Radiodating**

A quite different analytical use for radioisotopes is in the **dating** (i.e. determining the age) of rocks, fossils and sediments. In this technique it is assumed that the proportion of an element that is naturally radioactive has been the same throughout time. From the time of fossilisation or deposition the radioactive isotope will decay. By determining the amount of radioisotope remaining (or by examining the amount of a decay product) and from a knowledge of the half-life, it is possible to date the sample. For instance, if the radioisotope normally comprises 1% of the element and it is found that the sample actually contains 0.25% then two half-lives can be assumed to have elapsed since deposition. If the half-life is one million years then the sample can be dated as being two million years old.

For long-term dating, isotopes with long half-lives are necessary, such as  $^{235}\text{U}$ ,  $^{238}\text{U}$  and  $^{40}\text{K}$ , whereas for shorter-term dating  $^{14}\text{C}$  is widely used. It cannot be overemphasised that the assumptions made in radiodating are sweeping and hence palaeontologists and anthropologists who use this technique can give only approximate dates to their samples.

**14.6.3 Other applications****Molecular biology techniques**

Recent advances in molecular biology that have led to advances in genetic manipulation have depended heavily upon use of radioisotopes in DNA and RNA

**Table 14.10** Units commonly used to describe radioactivity

Unit	Abbreviation	Definition
Counts per minute or second	c.p.m. c.p.s.	The <i>recorded</i> rate of decay
Disintegrations per minute or second	d.p.m. d.p.s.	The <i>actual</i> rate of decay
Curie	Ci	The number of d.p.s. equivalent to 1 g of radium ( $3.7 \times 10^{10}$ d.p.s.)
Millicurie	mCi	$Ci \times 10^{-3}$ or $2.22 \times 10^9$ d.p.m.
Microcurie	$\mu$ Ci	$Ci \times 10^{-6}$ or $2.22 \times 10^6$ d.p.m.
Becquerel (SI unit)	Bq	1 d.p.s.
Terabecquerel (SI unit)	TBq	$10^{12}$ Bq or 27.027 Ci
Gigabecquerel (SI unit)	GBq	$10^9$ Bq or 27.027 mCi
Megabecquerel (SI unit)	MBq	$10^6$ Bq or 27.027 $\mu$ Ci
Electron volt	eV	The energy attained by an electron accelerated through a potential difference of 1 volt. Equivalent to $1.6 \times 10^{-19}$ J
Roentgen	R	The amount of radiation that produces $1.61 \times 10^{15}$ ion-pairs $\text{kg}^{-1}$
Rad	rad	The dose that gives an energy absorption of $0.01 \text{ J kg}^{-1}$
Gray	Gy	The dose that gives an energy absorption of $1 \text{ J kg}^{-1}$ . Thus $1 \text{ Gy} = 100 \text{ rad}$
Rem	rem	The amount of radiation that gives a dose in humans equivalent to 1 rad of X-rays
Sievert	Sv	The amount of radiation that gives a dose in humans equivalent to 1 Gy of X-rays. Thus $1 \text{ Sv} = 100 \text{ rem}$

sequencing, DNA replication, transcription, synthesis of complementary DNA, recombinant DNA technology and many similar studies. Many of these techniques are more fully discussed in Chapters 5 and 6.

### Clinical diagnosis

Radioisotopes are very widely used in medicine, in particular for diagnostic tests. Lung function tests routinely made using xenon-133 ( $^{133}\text{Xe}$ ) are particularly useful in diagnosis of malfunctions of lung ventilation. Kidney function tests using [ $^{133}\text{I}$ ]iodohippuric acid are used in diagnoses of kidney infections, kidney blockages or imbalance of function between the two kidneys.

Various aspects of haematology are also studied by using radioisotopes. These include such aspects as blood cell lifetimes, blood volumes and blood circulation times, all of which may vary in particular clinical conditions.

### Ecological studies

The bulk of radiotracer work is carried out in biochemical, clinical or pharmacological laboratories; nevertheless, radiotracers are also of use to ecologists. In particular, migratory patterns and behaviour patterns of many animals can be monitored using radiotracers. Another ecological application is in the examination of food chains where the primary producers can be made radioactive and the path of radioactivity followed throughout the resulting food chain.

### Sterilisation of food and equipment

Very strong  $\gamma$ -emitters are now widely used in the food industry for sterilisation of prepacked foods such as milk and meats. Normally either  $^{60}\text{Co}$  or  $^{137}\text{Cs}$  is used, but care has to be taken in some cases to ensure that the food product itself is not affected in any way. Thus doses often have to be reduced to an extent where sterilisation is not complete but nevertheless food spoilage can be greatly reduced.  $^{60}\text{Co}$  and  $^{137}\text{Cs}$  are also used in sterilisation of plastic disposable equipment such as Petri dishes and syringes, and in sterilisation of drugs that are administered by injection.

### Mutagens

Radioisotopes may cause mutations, particularly in microorganisms. In various microbiological studies mutants are desirable, especially in industrial microbiology. For instance, development of new strains of a microorganism that produce higher yields of a desired microbial product frequently involve mutagenesis by radioisotopes.

## 14.7 SUGGESTIONS FOR FURTHER READING

- BILLINGTON, D., JAYSON, G. G. and MALTBY, P. J. (1992). *Radioisotopes*. Bios Scientific, Oxford. (A description of principles and applications in the biosciences, for undergraduates and research workers.)
- CONNOR, K. J. and MCLINTOCK, I. S. (1994). *Radiation Protection Handbook for Laboratory Workers*. HHSC, Leeds. (A safety manual for laboratory work.)
- SLATER, R. J. (1996). Radioisotopes in molecular biology. In *Molecular Biology and Molecular Medicine*, ed. R. A. Myers, pp. 209–219. VCH, New York. (A summary of the application of radioisotopes to molecular biology.)
- SLATER, R. J. (2002). *Radioisotopes in Biology – A Practical Approach*, 2nd edn. Oxford University Press, Oxford. (A detailed account of the handling and use of radioactivity in biological research.)